

Feature Article

Polymer nanotechnology: Nanocomposites

D.R. Paul^{a,1}, L.M. Robeson^{b,*}^a Department of Chemical Engineering and Texas Materials Institute, University of Texas at Austin, Austin, TX 78712, United States^b Lehigh University, 1801 Mill Creek Road, Macungie, PA 18062, United States

ARTICLE INFO

Article history:

Received 19 February 2008

Received in revised form 2 April 2008

Accepted 4 April 2008

Available online 13 April 2008

Keywords:

Nanotechnology

Nanocomposites

Exfoliated clay

ABSTRACT

In the large field of nanotechnology, polymer matrix based nanocomposites have become a prominent area of current research and development. Exfoliated clay-based nanocomposites have dominated the polymer literature but there are a large number of other significant areas of current and emerging interest. This review will detail the technology involved with exfoliated clay-based nanocomposites and also include other important areas including barrier properties, flammability resistance, biomedical applications, electrical/electronic/optoelectronic applications and fuel cell interests. The important question of the “nano-effect” of nanoparticle or fiber inclusion relative to their larger scale counterparts is addressed relative to crystallization and glass transition behavior. Of course, other polymer (and composite)-based properties derive benefits from nanoscale filler or fiber addition and these are addressed.

© 2008 Elsevier Ltd. Open access under [CC BY-NC-ND license](http://creativecommons.org/licenses/by-nc-nd/3.0/).

1. Introduction

The field of nanotechnology is one of the most popular areas for current research and development in basically all technical disciplines. This obviously includes polymer science and technology and even in this field the investigations cover a broad range of topics. This would include microelectronics (which could now be referred to as nanoelectronics) as the critical dimension scale for modern devices is now below 100 nm. Other areas include polymer-based biomaterials, nanoparticle drug delivery, miniemulsion particles, fuel cell electrode polymer bound catalysts, layer-by-layer self-assembled polymer films, electrospun nanofibers, imprint lithography, polymer blends and nanocomposites. Even in the field of nanocomposites, many diverse topics exist including composite reinforcement, barrier properties, flame resistance, electro-optical properties, cosmetic applications, bactericidal properties. Nanotechnology is not new to polymer science as prior studies before the age of nanotechnology involved nanoscale dimensions but were not specifically referred to as nanotechnology until recently. Phase separated polymer blends often achieve nanoscale phase dimensions; block copolymer domain morphology is usually at the nanoscale level; asymmetric membranes often have nanoscale void structure, miniemulsion particles are below 100 nm; and interfacial phenomena in blends and composites involve nanoscale

dimensions. Even with nanocomposites, carbon black reinforcement of elastomers, colloidal silica modification and even naturally occurring fiber (e.g., asbestos-nanoscale fiber diameter) reinforcement are subjects that have been investigated for decades. Almost lost in the present nanocomposite discussions are the organic–inorganic nanocomposites based on sol–gel chemistry which have been investigated for several decades [1–3]. In essence, the nanoscale of dimensions is the transition zone between the macro-level and the molecular level. Recent interest in polymer matrix based nanocomposites has emerged initially with interesting observations involving exfoliated clay and more recent studies with carbon nanotubes, carbon nanofibers, exfoliated graphite (graphene), nanocrystalline metals and a host of additional nanoscale inorganic filler or fiber modifications.

This review will discuss polymer matrix based nanocomposites with exfoliated clay being one of the key modifications. While the reinforcement aspects of nanocomposites are the primary area of interest, a number of other properties and potential applications are important including barrier properties, flammability resistance, electrical/electronic properties, membrane properties, polymer blend compatibilization. An important consideration in this review involves the comparison of properties of nanoscale dimensions relative to larger scale dimensions. The synergistic advantage of nanoscale dimensions (“nano-effect”) relative to larger scale modification is an important consideration. Understanding the property changes as the particle (or fiber) dimensions decrease to the nanoscale level is important to optimize the resultant nanocomposite. As will be noted, many nanocomposite systems noted in the literature can still be modeled using continuum models where absolute size is not important since only shape and volume fraction

* Corresponding author. Tel.: +1 610 481 0117.

E-mail addresses: drp@che.utexas.edu (D.R. Paul), lesrob2@verizon.net (L.M. Robeson).¹ Tel.: +1 512 471 5392.

loading are necessary to predict properties. Nanoscale is considered where the dimensions of the particle, platelet or fiber modification are in the range of 1–100 nm. With the platelet or fiber, the smallest dimension is considered for that range (platelet thickness or fiber diameter).

2. Fundamental considerations

In the area of nanotechnology, polymer matrix based nanocomposites have generated a significant amount of attention in the recent literature. This area emerged with the recognition that exfoliated clays could yield significant mechanical property advantages as a modification of polymeric systems [4–6]. The achieved results were at least initially viewed as unexpected (“nano-effect”) offering improved properties over that expected from continuum mechanics predictions. More recent results have, however, indicated that while the property profile is interesting, the clay-based nanocomposites often obey continuum mechanics predictions. There are situations where nanocomposites can exhibit properties not expected with larger scale particulate reinforcements.

It is now well-recognized that the crystallization rate and degree of crystallinity can be influenced by crystallization in confined spaces. In these cases, the dimensions available for spherulitic growth are confined such that primary nuclei are not present for heterogeneous crystallization and homogeneous nucleation thus results. This results in the value of n in the Avrami equation approaching one and often leads to reduced crystallization rate, degree of crystallinity and melting point. This has been observed in phase separated block copolymers [7,8] and has also been observed in polymer blends [9]. Confined crystallization of linear polyethylene in nanoporous alumina showed homogeneous nucleation with pore diameters of 62–110 nm but heterogeneous nucleation for 15–48 nm pores [10]. Linear polyethylene [11] and syndiotactic polystyrene [12] in nanoporous alumina both showed decreased crystallinity versus bulk crystallization. With nanoparticle incorporation in a polymer matrix, similarities to confined crystallinity (as noted above for crystallization in nanopores) exist as well as nucleation effects and disruption of attainable spherulite size.

With inorganic particle and nanoparticle inclusions, nucleation of crystallization can occur. At the nanodimension scale, the nanoparticle can substitute for the absence of primary nuclei thus competing with the confined crystallization. At higher nanoparticle content, the increased viscosity (decreased chain diffusion rate) can lead to decreased crystallization kinetics. Thus, the crystallization process is complex and influenced by several competing factors. Nucleation of crystallization (at low levels of addition) evidenced by the onset temperature of crystallization (T_c) and crystallization half-time has been observed in various nanocomposites (poly(ϵ -caprolactone)–nanoclay [13], polyamide 66–nanoclay [14,15], polylactide–nanoclay [16], polyamide 6–nanoclay [17], polyamide 66–multi-walled carbon nanotube [18], polyester–nanoclay [19],

poly(butylene terephthalate)–nanoclay [20], polypropylene–nanoclay (sepiolite) [21], polypropylene/multi-walled carbon nanotube [22]). At higher levels of nanoparticle addition, retardation of the crystallization rate has been observed even in those systems where nucleation was observed at low levels of nanoparticle incorporation [15,18,20,22–24]. The higher level of nanoparticle inclusion was noted to yield retardation of crystallization due to diffusion constraints. This was also apparent in a study where unmodified and organically modified clay were incorporated in maleic anhydride grafted polypropylene [25]. Nucleation was observed with unmodified clay, whereas the exfoliated clay yielded a reduced crystallization rate. A recent review of the crystallization behavior of layered silicate clay nanocomposites noted that while nucleation is observed in many systems the overall crystallization rate is generally reduced particularly at higher levels of nanoclay addition [26].

Another “nano-effect” noted in the literature has been the change in the T_g of the polymer matrix with the addition of nano-sized particles. Both increases and decreases in the T_g have been reported dependant upon the interaction between the matrix and the particle. In essence, if the addition of a particle to an amorphous polymer leads to a change in the T_g , the resultant effect on the composite properties would be considered a “nano-effect” and not predictable employing continuum mechanics relationships unless the T_g changes were properly accounted for or were quite minor. The glass transition of a polymer will be affected by its environment when the chain is within several nanometers of another phase. An extreme case of this is where the other environment is air (or vacuum). It has been well-recognized in the literature that the T_g of a polymer at the air–polymer surface or thin films (<100 nm) may be lower than that in bulk [27]. This can also be considered a confinement effect. A specific experimental example was reported where poly(2-vinyl pyridine) showed an increase in T_g , poly(methyl methacrylate) (PMMA) showed a decrease in T_g and polystyrene showed no change with silica nanosphere incorporation. These differences were ascribed to surface wetting [28]. The T_g decrease for PMMA was ascribed to free volume existing at the polymer surface interface due to poor wetting. In most literature examples where T_g values have been obtained, usually only modest changes are reported (<10 °C) as noted in various examples tabulated in Table 1. In some cases the organic modification of clay can result in a decrease in T_g due to plasticization [29]. It should be noted that the values noted in Table 1 involved relatively low levels of nanoparticle incorporation (<0.10 wt fraction and even lower volume fraction) and larger changes in T_g could be expected at much higher volume fraction loadings. For crosslinked polymers, another consideration is necessary as the presence of nanoparticles could yield a crosslink density change over the unmodified composite. This could be due to preferential interactions of the crosslinking agent with the nanoparticle surface or interruption of the crosslink density due to confinement effects. A theoretical model has been

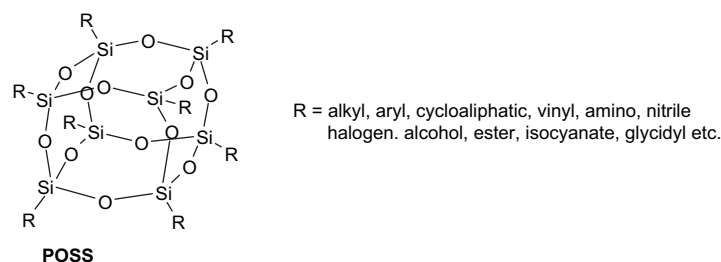
Table 1
Glass transition changes with nanofiller incorporation

Polymer	Nanofiller	T_g change (°C)	Reference
Polystyrene	SWCNT	3	[34]
Polycarbonate	SiC (0.5–1.5 wt%) (20–60 nm particles)	No change	[35]
Poly(vinyl chloride)	Exfoliated clay (MMT) (<10 wt%)	–1 to –3	[36]
Poly(dimethyl siloxane)	Silica (2–3 nm)	10	[37]
Poly(propylene carbonate)	Nanoclay (4 wt%)	13	[38]
Poly(methyl methacrylate)	Nanoclay (2.5–15.1 wt%)	4–13	[39]
Polyimide	MWCNT (0.25–6.98 wt%)	–4 to 8	[40]
Polystyrene	Nanoclay (5 wt%)	6.7	[41]
Natural rubber	Nanoclay (5 wt%)	3	[42]
Poly(butylene terephthalate)	Mica (3 wt%)	6	[43]
Polylactide	Nanoclay (3 wt%)	–1 to –4	[29]

SWCNT = single-walled carbon nanotubes; MMT = montmorillonite; MWCNT = multi-walled carbon nanotubes.

developed to predict the glass transition temperature of nanocomposites [30]. The model predicts both increases and decreases in T_g dependant upon specific interactions and shows good agreement with the experimental data noted above [28].

A situation does exist where significant increases in the glass transition temperature have been noted involving polyhedral oligomeric silsesquioxane (POSS) cage structures chemically reacted into the polymeric network [31–34]. These cage structures with a particle diameter in the range of 1–3 nm can be functionalized to provide chemical reactivity with various polymer systems. Examples include octavinyl (R = vinyl group) incorporation for copolymerization with PMMA [31], amine groups for incorporation into polyamides [32] and polyimides [33]. This parallels the glass transition increase often noted in the sol–gel inorganic–organic networks.



While the glass transition temperature and crystallinity are the major property changes of interest of the nanocomposite polymer matrix, other “nano-effects” or property improvements over larger scale dimensions can be observed. Disruption of packing of rigid chain polymers resulting in higher free volume has been observed in permeability studies [44], surface area effects in photovoltaic applications involving conjugated polymers, surface area effects for catalysts incorporated in polymers, polymer chain dimensions where the radius of gyration is greater than the distance between adjacent nanoparticles, optical properties, nanofiber scaffolds for tissue engineering are additional areas. The “aging” of polymers is a thickness dependant property with rapid change at nanoscale dimensions [45,46]. This property is due to the ability of free volume to diffuse out of the sample and the diffusion coefficient (although very low) becomes important in the time scale associated with polymer utility (days to years) at nanoscale thicknesses. Surface area effects including catalysts, bioactivity, often require nanolevel dimensions to achieve optimum performance.

This review of polymer matrix based nanocomposites is divided into two major sections: clay-based nanocomposites with emphasis on mechanical reinforcement and other property modifications. Mechanical enhancement is usually associated with polymer-based composites, however, a number of other areas have emerged where additional property enhancements can be realized by incorporation of nanoscale particles, platelets or fibers.

3. Clay-based polymer nanocomposites

3.1. Structure of montmorillonite

The clay known as montmorillonite consists of platelets with an inner octahedral layer sandwiched between two silicate tetrahedral layers [47] as illustrated in Fig. 1. The octahedral layer may be

thought of as an aluminum oxide sheet where some of the aluminum atoms have been replaced with magnesium; the difference in valences of Al and Mg creates negative charges distributed within the plane of the platelets that are balanced by positive counterions, typically sodium ions, located between the platelets or in the galleries as shown in Fig. 1. In its natural state, this clay exists as stacks of many platelets. Hydration of the sodium ions causes the galleries to expand and the clay to swell; indeed, these platelets can be fully dispersed in water. The sodium ions can be exchanged with organic cations, such as those from an ammonium salt, to form an organoclay [48–57]. The ammonium cation may have hydrocarbon tails and other groups attached and is referred to as a “surfactant” owing to its amphiphilic nature. The extent of the negative charge of the clay is characterized by the cation exchange capacity, i.e., CEC.

The X-ray d -spacing of completely dry sodium montmorillonite is 0.96 nm while the platelet itself is about 0.94 nm thick [47,58]. When the sodium is replaced with much larger organic surfactants, the gallery expands and the X-ray d -spacing may increase by as

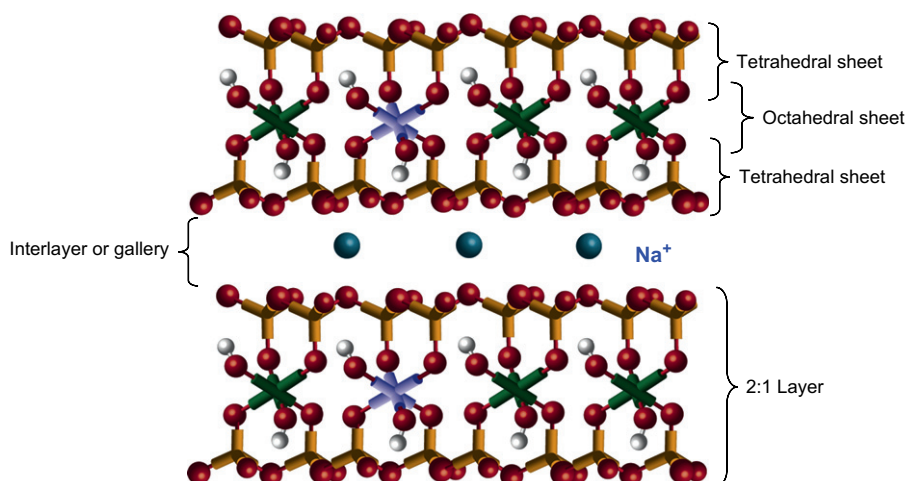


Fig. 1. Structure of sodium montmorillonite. Courtesy of Southern Clay Products, Inc.

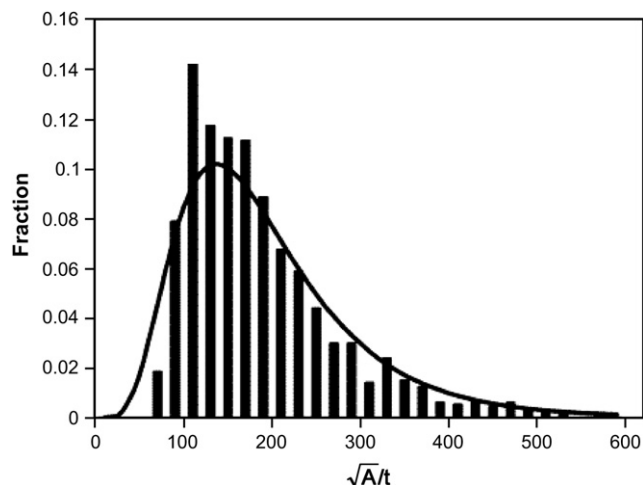


Fig. 2. Aspect ratio distribution of native sodium montmorillonite platelets [61]. Reproduced with permission of the American Chemical Society.

much as 2 to 3-fold [59,60]. While the thickness of montmorillonite platelets is a well-defined crystallographic dimension, the lateral dimensions of the platelets are not. They depend on how the platelets grew from solution in the geological process that formed them. Many authors grossly exaggerate the lateral size with dimensions quoted of the order of microns or even tens of microns. A commonly used montmorillonite was accurately characterized recently by depositing platelets on a mica surface from a very dilute suspension and then measuring the lateral dimensions by atomic force microscopy [61]. Since the platelets are not uniform or regular in lateral size or shape, the platelet area, A , was measured and its square-root was normalized by platelet thickness, t , to calculate an “aspect ratio”. The distribution of aspect ratios found is shown in Fig. 2. If each platelet were circular with diameter D , then \sqrt{A}/t would be $\sqrt{\pi/4}(D/t) = 0.89(D/t)$. Since t is approximately 1 nm, Fig. 2 shows that the most probable lateral dimension is in the range of 100–200 nm.

3.2. Nanocomposite formation: exfoliation

Nanocomposites can, in principle, be formed from clays and organoclays in a number of ways including various *in situ* polymerization [4,6,62–68], solution [51,53], and latex [69,70] methods. However, the greatest interest has involved melt processing [71–139] because this is generally considered more economical, more flexible for formulation, and involves compounding and fabrication facilities commonly used in commercial practice. For most purposes, complete exfoliation of the clay platelets, i.e., separation of platelets from one another and dispersed individually in the polymer matrix, is the desired goal of the formation process. However, this ideal morphology is frequently not achieved and varying degrees of dispersion are more common. While far from a completely accurate or descriptive nomenclature, the literature commonly refers to three types of morphology: immiscible (conventional or microcomposite), intercalated, and miscible or exfoliated. These are illustrated schematically in Fig. 3 along with example transmission electron microscopic, TEM, images and the expected wide angle X-ray scans [48–53,83].

For the case called “immiscible” in Fig. 3, the organoclay platelets exist in particles comprised of tactoids or aggregates of tactoids more or less as they were in the organoclay powder, i.e., no separation of platelets. Thus, the wide angle X-ray scan of the polymer composite is expected to look essentially the same as that obtained for the organoclay powder; there is no shifting of the X-ray d -spacing. Generally, such scans are made over a low range

of angles, 2θ , such that any peaks from a crystalline polymer matrix are not seen since they occur at higher angles. For completely exfoliated organoclay, no wide angle X-ray peak is expected for the nanocomposite since there is no regular spacing of the platelets and the distances between platelets would, in any case, be larger than what wide angle X-ray scattering can detect.

Often X-ray scans of polymer nanocomposites show a peak reminiscent of the organoclay peak but shifted to lower 2θ or larger d -spacing. The fact that there is a peak indicates that the platelets are not exfoliated. The peak shift indicates that the gallery has expanded, and it is usually assumed that polymer chains have entered or have been intercalated in the gallery. Placing polymer chains in such a confined space would involve a significant entropy penalty that presumably must be driven by an energetic attraction between the polymer and the organoclay [76–79]. It is possible that the gallery expansion may in some cases be caused by intercalation of oligomers or low molecular weight polymer chains. The early literature seemed to suggest that “intercalation” would be useful and perhaps a precursor to exfoliation. Subsequent research has suggested alternative ideas about how the exfoliation process may occur in melt processing and how the details of the mixing equipment and conditions alter the state of dispersion achieved [54,82,84,140]. These ideas are summarized in the cartoon shown in Fig. 4 [84]. As made commercially, the particles of an organoclay powder are about 8 μm in size and consist of aggregates of tactoids, or stacks of platelets; the stresses imposed during melt mixing break up aggregates and can shear the stack into smaller ones as suggested in Fig. 4. However, there evidently is a limit to how finely the clay can be dispersed just by mechanical forces. If the polymers and organoclay have an “affinity” for one another, the contact between polymers and organoclay can be increased by peeling the platelets from these stacks one by one until, given enough time in the mixing device, all the platelets are individually dispersed as suggested in Fig. 4. This notion is supported by many TEM images at various locations in the extruder and is more plausible than imagining the polymer chains diffusing into the galleries, i.e., intercalation, and eventually pushing them further and further apart until an exfoliated state is reached.

The nature of the extruder and the screw configuration are important to achieve good organoclay dispersion [83]. Longer residence times in the extruder favor better dispersion [83]. In some cases, having a higher melt viscosity is helpful in achieving dispersion apparently because of the higher stresses that can be imposed on the clay particles [84,126]; however, this effect is not universally observed. The location of where the organoclay is introduced into the extruder has also been shown to be important [120]. However, no matter how well these process considerations are optimized, it is clear that complete exfoliation, or nearly so, cannot be achieved unless there is a good thermodynamic affinity between the organoclay and the polymer matrix. This affinity can be affected to a very significant extent by optimizing the structure of the surfactant used to form the organoclay [85,88,99,100,109,113,119,141] and possibly certain features of the clay itself like its CEC [115], as this affects the density of surfactant molecules over the silicate surface.

A key factor in the polymer–organoclay interaction is the affinity polymer segments have for the silicate surface [84,85,94,113,141,142]. Nylon 6 appears to have good affinity for the silicate surface, perhaps by hydrogen bonding, and as a result very high levels of exfoliation can be achieved in this matrix provided the processing conditions and melt rheology are properly selected [83,84,120]. Surfactants with a single long alkyl tail give the best exfoliation [141]. As more long chain alkyls are added to the surfactant, the extent of exfoliation is decreased [141]. It has been proposed that at least one alkyl tail is needed to reduce the platelet–platelet cohesion while adding more than one tends to block

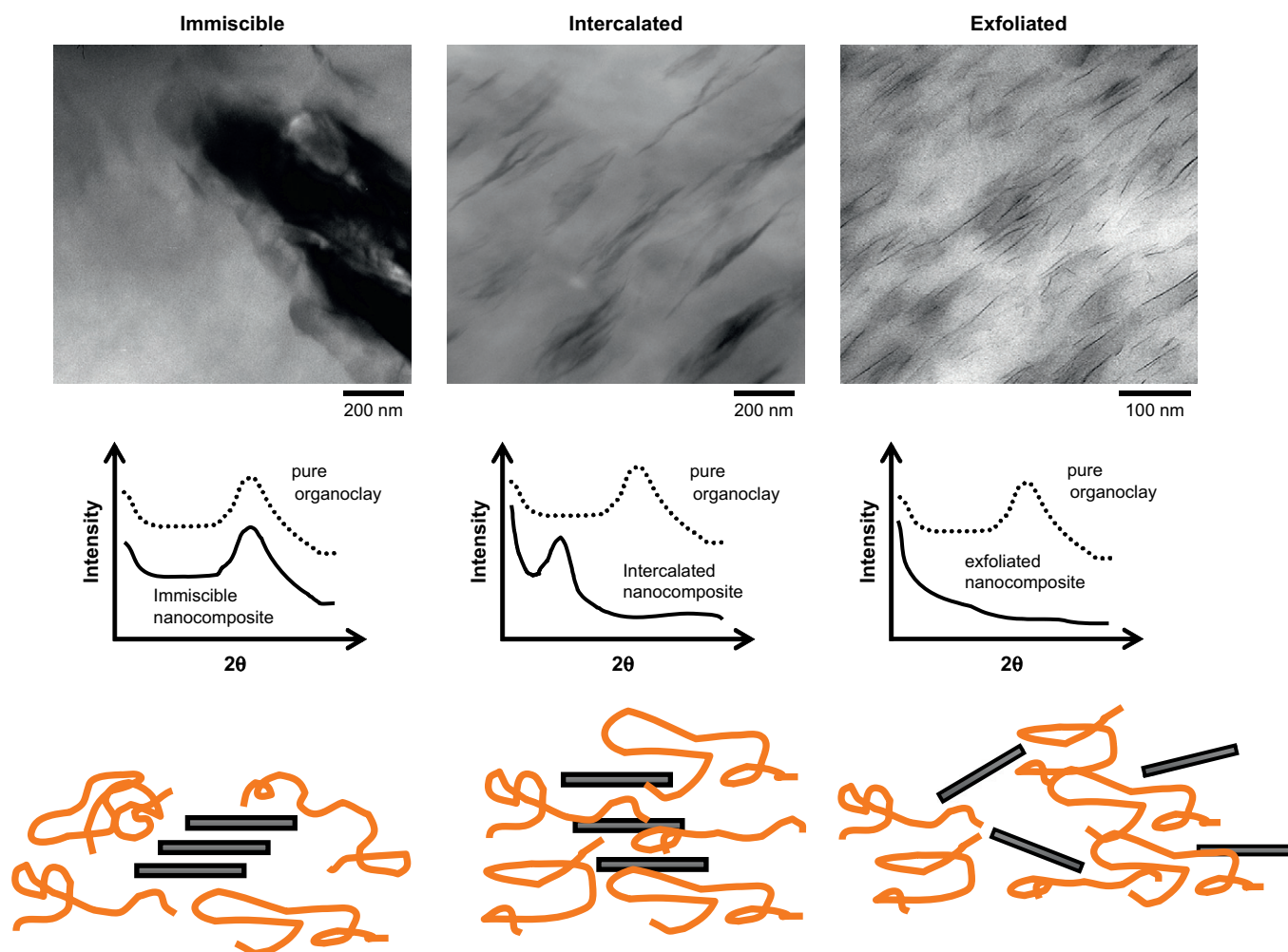


Fig. 3. Illustration of different states of dispersion of organoclays in polymers with corresponding WAXS and TEM results.

access of the polyamide chains from the silicate surface diminishing these favorable interactions while increasing the very unfavorable alkyl–polyamide interaction. On the other hand, non-polar polyolefin segments have no attraction to the polar silicate surface, and in this case, increasing the number of alkyls on the surfactant improves dispersion of the organoclay in the polyolefin matrix since

a larger number of alkyls decrease the possible frequency of the unfavorable polyolefin–silicate interaction and increases the frequency of more favorable polyolefin–alkyl contacts [96,100,105].

Even under the best of circumstances exfoliation of organoclays in neat polyolefins like polypropylene, PP, or polyethylene, PE, is not very good and far less than that observed in polyamides,

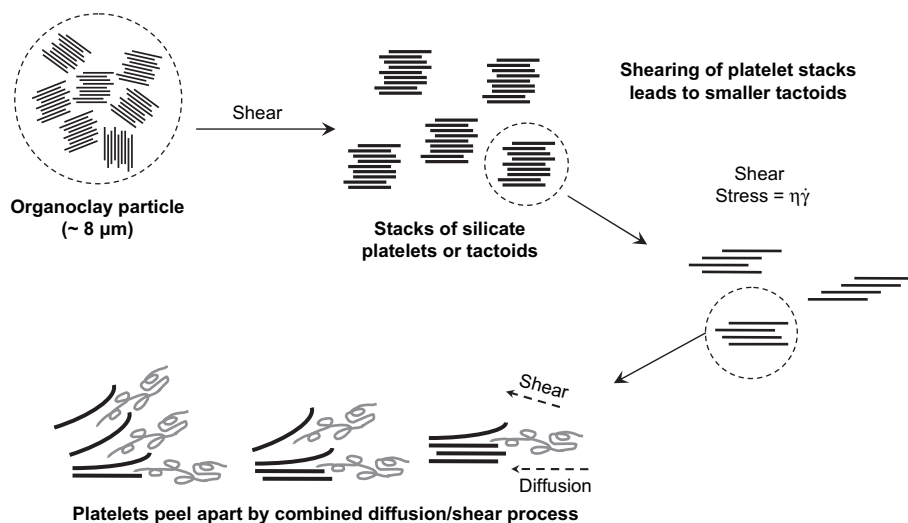


Fig. 4. Mechanism of organoclay dispersion and exfoliation during melt processing [84]. Reproduced with permission of Elsevier Ltd.

polyurethanes, and some other polar polymers [84,96,101]. It has been found that a small amount of a polyolefin that has been lightly grafted with maleic anhydride, ~1% MA by weight is typical, can act as a very effective “compatibilizer” for dispersing the organoclay in the parent polyolefin [84,101,103,106,117,118,143–148]. This does not lead to the high level of exfoliation that can be achieved in polyamides, but this approach has allowed such nanocomposites to move forward in commercial applications, particularly in automotive parts [54,99,106].

In the case of olefin copolymers with polar monomers like vinyl acetate and methacrylic acid (and corresponding ionomers), the degree of exfoliation that can be achieved progressively improves as the polar monomer content increases [113,119]. In all cases, the best exfoliation is achieved when the structure of the surfactant and the process parameters are optimized.

3.3. Characterization of nanocomposite morphology

An important issue is to relate the performance of nanocomposites to their morphological structure; experimental evaluation of performance is certainly easier than characterization of their morphology. Wide angle X-ray scattering, WAXS, is frequently used because such analyses are relatively simple to do. However, such analyses can be misleading and are not quantitative [149–151]. As indicated in Fig. 3, the organoclay has a characteristic peak indicative of the platelet separation or *d*-spacing; other peaks may be seen resulting from multiple reflections as predicted by Bragg's law. The presence of the same peak in the nanocomposite is irrefutable evidence that the nanocomposite contains organoclay tactoids as suggested in Fig. 3. However, the absence of such a peak is not conclusive evidence for a highly exfoliated structure as has been repeatedly pointed out in the literature [151]; many factors must be considered to interpret WAXS scans. If the sensitivity, or counting time, of the scan is low, then an existing peak may not be seen. When the tactoids are internally disordered or not well aligned to one another, the peak intensity will be low and may appear to be completely absent. These issues can be well illustrated by analyses of polyolefin nanocomposites, which are never fully exfoliated, that have been injection molded. X-ray scans of the molded surface reveal a peak indicating the presence of tactoids. However, after milling away the surface of these specimens, subsequent scans of the milled surface in the core of the bar may not reveal a peak because the tactoids are more randomly oriented in the interior than near the as-molded surface [103,118]. However, if a more sensitive scan is made, the peak can usually be seen.

In some cases, the WAXS scan may reveal a shift in the peak location relative to that of the neat organoclay. The peak may shift to lower angles, or larger *d*-spacing, and is generally taken as evidence of “intercalation” of polymers (or perhaps other species) into the galleries [48–53,73,79]. However, an opposite shift may also

occur, and this is usually attributed to loss of unbound surfactant from the gallery or to surfactant degradation [89,107]. All of these processes may occur simultaneously rendering uncertainty in the interpretation. In any case, intercalation per se does not seem to be a contributor to develop useful nanocomposite performance.

Small angle X-ray scattering, SAXS, can be more informative and somewhat quantitative as explained by numerous authors [17,152–156]. However, this technique has not been widely used except in a few laboratories probably because most laboratories do not have SAXS facilities or experience in interpreting the results. Other techniques like solid-state NMR and neutron scattering have also been used on a limited basis to explore clay dispersion [95,157–162].

A far more direct way of visualizing nanocomposite morphology is via transmission electron microscopy, TEM; however, this approach requires considerable skill and patience but can be quantitative. Use of TEM is often criticized because it reveals the morphology in such a small region. However, this can be overcome by taking images at different magnifications and from different locations and orientations until a representative picture of the morphology is established. The major obstacle in obtaining good TEM images is not in the operation of the microscope but in microtoming sections that are thin and uniform enough to reveal the morphology. Fortunately, the elemental composition of the clay compared to that of the polymer matrix is such that no staining is required. When exfoliation is essentially complete, as in the case of nylon 6, one can see the ~1 nm thick clay platelets as dark lines when the microtome cut is perpendicular to the platelets. Image analysis can be used to quantify the distribution of platelet lengths, but meaningful statistics require analyzing several hundred particles [58,84,93,119]. However, it must be remembered that the dimensions observed reflect a random cut through an irregular platelet and only rarely will the maximum dimension be seen [163,164]. Thus, the aspect ratio distribution seen in this way will lead to smaller values than true dimensions like those given by Fig. 2.

Even for the best nylon 6 nanocomposites, exfoliation is generally never complete and one can see particles consisting of two, three or more platelets [58]. In some cases, these platelets may be skewed relative to one another as suggested in Fig. 5 [93]. Thus, some particles may appear to be longer than the platelets really are. These kinds of issues should be kept in mind when interpreting quantitative analyses of particle aspect ratios and in comparison of observed performance with that predicted by composite theory [58].

Nanocomposites made from polyolefins, styrenics, and other polymers that lead to lower degrees of exfoliation reveal particles much thicker than single clay platelets as expected [101,110,111,117,119]. However, the clay particles are also much longer than the individual clay platelets indicated in Fig. 2. As the

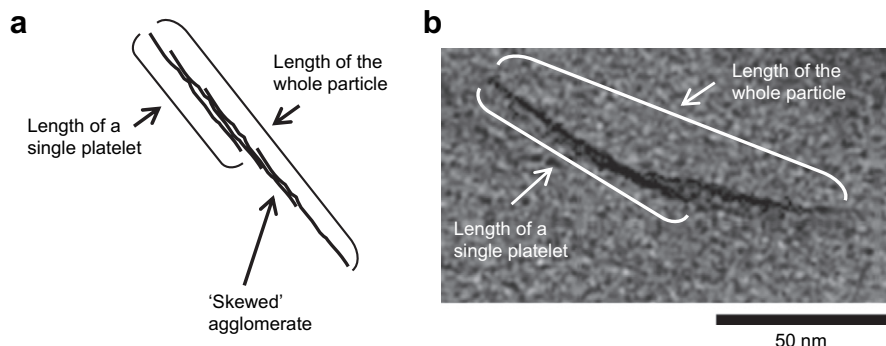


Fig. 5. Examples of skewed platelets such that particles appear longer than platelets of MMT [93]. Reproduced with permission of Elsevier Ltd.

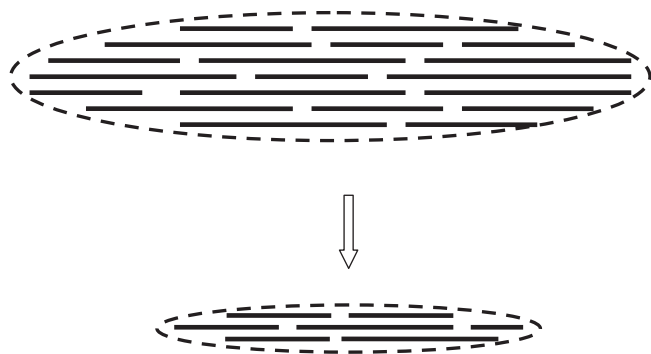


Fig. 6. A more realistic picture of clay tactoids and how they become shorter as the level of dispersion increases.

polymer–organoclay affinity is increased by adding a compatibilizer, e.g., PP-g-MA or PE-g-MA, or increasing the content of a polar comonomer, e.g., vinyl acetate, the clay particles not only become thinner (fewer platelets in the stack) but also become shorter [103,106,117–120]. However, generally the particle thickness decreases more rapidly than the length such that the aspect ratio increases; this generally improves performance.

The fact that the particles become shorter does not mean that clay platelets are breaking or being attributed during processing, although, this may occur under some extreme conditions [120]. Instead, considerable evidence indicates that the vision of tactoids as usually drawn, see Figs. 3 and 4, where the platelets are all of the same length and in registry with one another is not correct. Fig. 6 shows a more realistic vision of a tactoid where the particle length can be much longer than individual platelets and how these particles evolve as dispersion improves [106,117].

Complications arise when calculating an average aspect ratio of particles when there is a distribution of both length and thickness. First, one can calculate a number average, a weight average, or other weightings of the distribution [58,113,119]. Second, one can average the aspect ratios or average separately the lengths and thickness and calculate an aspect ratio from these averages [113,119]. There is no theoretical guidance on which is the better predictor of performance or for use in composite modeling [113,117,119].

To take full advantage of the reinforcement or tortuosity clay platelets or particles can provide to mechanical and thermal or barrier properties of nanocomposites, they must be oriented in the appropriate direction and not curled or curved. The alignment of particles is affected by the type of processing used to form the test specimen, e.g., extrusion, injection molding, etc. This is a separate issue from the degree of dispersion or exfoliation which is usually determined in the mixing process. Techniques like compression molding usually do not lead to good alignment or straightening of the high aspect ratio particles, and measurements made on such specimens often underestimate the potential performance. TEM can be used to assess and even quantify particle orientation and curvature and this information can, in principle, be factored into appropriate models to ascertain their effect on performance [86,110,131,134,138].

3.4. Nanocomposite mechanical properties: reinforcement

A common reason for adding fillers to polymers is to increase the modulus or stiffness via reinforcement mechanisms described by theories for composites [58,165–185]. Properly dispersed and aligned clay platelets have proven to be very effective for increasing stiffness. This is illustrated in Fig. 7 by comparing the increase in the tensile modulus, E , of injection molded composites based on nylon 6, relative to the modulus of the neat polyamide matrix, E_m , when

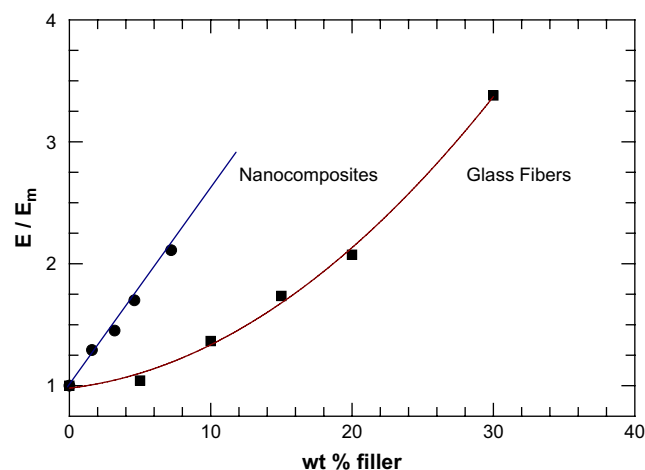


Fig. 7. Comparison of modulus reinforcement (relative to matrix polymer) increases for nanocomposites based on MMT versus glass fiber (aspect ratio ~ 20) for a nylon 6 matrix [58]. Reproduced by permission of Elsevier Ltd.

the filler is an organoclay versus glass fibers [58]. In this example, increasing the modulus by a factor of two relative to that of neat nylon 6 requires approximately three times more mass of glass fibers than that of montmorillonite, MMT, platelets. Thus, the nanocomposite has a weight advantage over the conventional glass fiber composite. Furthermore, if the platelets are aligned in the plane of the sample, the same reinforcement should be seen in all directions within the plane, whereas fibers reinforce only along a single axis in the direction of their alignment [165]. In addition, the surface finish of the nanocomposite is much better than that of the glass fiber composite owing to nanometer size of the clay platelets versus the 10–15 μ diameter of the glass fibers. A central question is whether the greater efficiency of the clay has anything to do with its nanometric dimensions, i.e., a “nano-effect”. To answer this requires considering many issues which we will do later in this section; however, the short answer is that we can explain essentially all of the experimental trends using composite theory without invoking any “nano-effects” [58].

Fig. 8 shows an analogous comparison of nanocomposites based on thermoplastic polyolefin or TPO matrix, polypropylene plus an ethylene-based elastomer, with conventional talc-filled TPO [103]. The latter is widely used in automotive applications; however, in some cases, they are being replaced with TPO nanocomposites. In

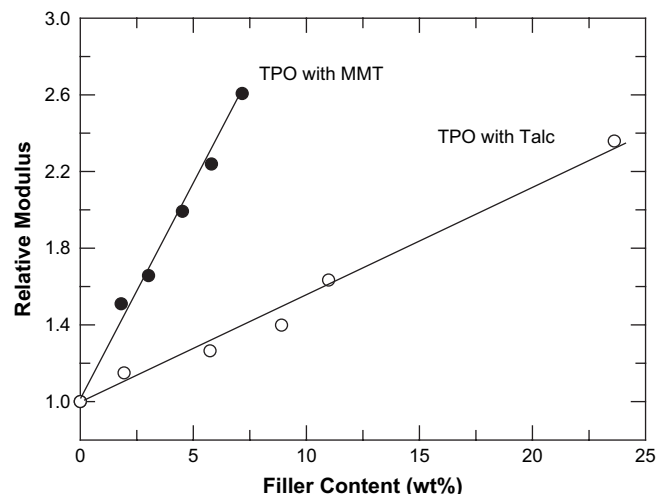


Fig. 8. Comparison of modulus reinforcement for nanocomposites based on MMT versus talc for a TPO matrix [103]. Reproduced by permission of Elsevier Ltd.

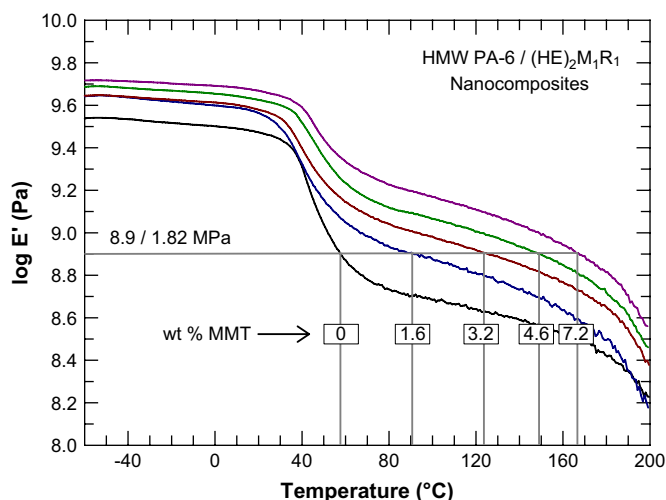


Fig. 9. Experimental storage modulus data versus temperature for nylon 6 nanocomposites. The horizontal line is used to estimate the heat distortion temperature (HDT) at an applied stress of 1.82 MPa or 264 psi [58]. Reproduced by permission of Elsevier Ltd.

this case, doubling the modulus of the TPO requires more than four times more talc than MMT; this presents a weight, and consequently fuel, savings along with the improved surface finish [103,106]. The polyamide nanocomposites in Fig. 7 are very highly exfoliated, whereas the exfoliation of the clay in the TPO of Fig. 8 is not nearly so perfect [103,106,117,118]. However, it should be recognized that the talc particles do not have as high aspect ratio as the glass fibers used in these comparisons [58,186]. Another factor at play here is the lower modulus of TPO than nylon 6. The lower the matrix modulus, the greater is the relative increase in reinforcement caused by adding a filler [94].

Fig. 9 shows dynamic mechanical moduli of the nylon 6 nanocomposites from Fig. 7 versus temperature. The intersection of these curves with the horizontal line shown is a good approximation to the heat distortion temperature, HDT, of these materials [58]. This temperature, used as a benchmark for many applications, can be increased by approximately 100 °C by addition of about 7% by weight of MMT. This effect has been explained by simple reinforcement, as predicted by composite theory, without invoking any special “nano-effects”; the effect of MMT on the glass transition of these materials is very slight if any at all [58]. Indeed, glass fibers cause an analogous increase in HDT.

Addition of fillers, including clay, can also increase strength as well as modulus [84]; however, the opposite may also occur [99]. A main issue is the level of adhesion of the filler to the matrix. For glass fiber composites, chemical bonding at the interface using silane chemistry is used to achieve high strength composites [186]. On the other hand, the modulus of glass fiber composites is not very much affected by the level of interfacial adhesion [186]. Unfortunately, at this time there is no effective way to measure the level of adhesion of clay particles with polymer matrices. In addition, there are no effective methods at this time to create chemical bonds between clay particles and polymer matrices analogous to those used for glass fibers. Generally, addition of organoclays to ductile polymers increases the yield strength; however, for brittle matrices failure strength is typically decreased [84,99–101].

Addition of fillers generally decreases the ductility of polymers, e.g., elongation at break. For glass fibers, talc, etc. this is well known and expected. Similar trends are also seen for nanocomposites [84,100], but this seems to have been unexpected and disappointing to some working in this field. Impact strength is an energy measurement, i.e., a force acting through a distance. A reduced

elongation at break often means a reduced energy to break but there are exceptions to this [84,100,116]. Addition of clay may increase the stress levels via reinforcement more than the reduction in deformation as recently demonstrated for some nanocomposites [116]. Generally speaking, the reduction in ductility or energy to break is more severe when the polymer matrix is below its glass transition, whereas the effects of adding clay may not be so dramatic when the matrix is above its glass transition temperature [82,84,100,119]. This involves a shift in fracture mechanisms that is beyond the scope of this review.

Melt rheological properties of polymers can be dramatically altered in the low shear rate or frequency region such that these fluids appear to have a yield stress [84,117,118,187–189]. The effects in the high shear rate region are usually much less dramatic [84]. A great deal has been written about these effects and their causes, and this will not be reviewed here. Interestingly, the addition of clay seems to be an effective way to increase “melt strength” which can be useful in some polymer processing operations like film blowing or blow molding [54,96].

To answer the question of whether the large increase in modulus caused by clay platelets or particles relative to conventional fillers, like that illustrated in Figs. 7 and 8, is due to some “nano-effect”, one must first determine whether effects of this magnitude can be predicted by composite theories. That is, by a “nano-effect”, we mean some change in the local properties of the matrix caused by the extremely high surface area filler and the small distances between nanofiller particles even at low mass loadings. It is well known that clay particles are effective nucleating agents which greatly change the crystalline morphology and crystal type for polymers like nylon 6 or PP [87]. Potential “confinement” effects are also discussed in the context of nanocomposites.

A basic premise of composite theories is that the matrix and filler have the same properties as when the other component is not there. These theories, thus, only predict the effects of simple reinforcement and do not allow for any “nano-effects” of the type mentioned. Clearly, reinforcement does occur and the issue is whether that alone can explain the observations or not. Composite theories consider only the aspect ratio, orientation and volume fraction of filler in the matrix; the absolute filler particle size does not enter into the calculations. We have already mentioned the difficulties of experimentally determining the aspect ratio (sectioning issues, averaging of distributions, etc.). Furthermore, determining what values to assign to the properties of the clay platelets (like its modulus) is not trivial. Finally, the various composite theories differ somewhat in their predictions owing to the assumptions and simplifications used in their mathematical formulation. These and other issues are worth remembering as we proceed with their analysis using data for nylon 6 nanocomposites.

We wish to compare composite calculations with experimental data for the modulus of nylon 6 nanocomposites where the degree of exfoliation is very high but not perfect. An image analysis of many TEM photomicrographs was used to construct a platelet length distribution which looks very similar to that in Fig. 2 [58]; the number average platelet length was found to be 91 nm. While the majority of the clay particles was single platelets (thickness ~ 0.94 nm), there were some doublets, some triplets, and a few quadruplets. It was estimated, by a rather involved analysis, that the number average platelet thickness was 1.61 nm [58]. Thus, an upper bound on the aspect ratio for perfect exfoliation (using number averages of the distribution) would be about $91/0.94 = 97$ while a more realistic estimate might be $91/1.61 = 57$.

Next, we need the in-plane modulus of a montmorillonite platelet. Information from a variety of sources suggests that a reasonable value is 178 GPa [58,190]; however, some molecular dynamics calculations suggest significantly larger values [191]. A density for MMT of 2.83 g/cm³ was used to convert weight fractions

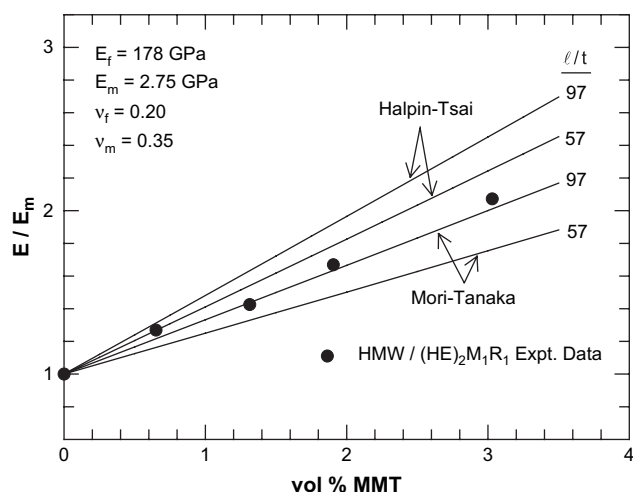


Fig. 10. Experimental and theoretical stiffness data for nylon 6 nanocomposites; model predictions are based on unidirectional reinforcement of pure MMT having a filler modulus of 178 GPa and aspect ratio of 57 (experimentally determined number average value) and 97, corresponding to complete exfoliation. Note that experimental modulus data are plotted versus vol% MMT since MMT is the reinforcing agent [58]. Reproduced by permission of Elsevier Ltd.

to volume fractions. The properties of the matrix (modulus, Poisson ratio, density, etc.) were experimentally measured values [58]. The equations of Halpin–Tsai [168] and Mori–Tanaka [167] are frequently used for composite calculations; the former predicts higher levels of reinforcement for the cases of interest here than the latter as seen in Fig. 10. Interestingly, the predictions via these two theories and the two estimates of aspect ratio give results that bracket the experimental data. Thus, we conclude that simple reinforcement considerations adequately explain the observations given all the issues involved in making these calculations. Any “nano-effect” is relatively minor if at all.

More needs to be said about the comparisons shown in Figs. 7 and 8. The aspect ratio of the glass fibers in the nylon 6 matrix is about 20, whereas the aspect ratio of MMT platelets is 3–5 times larger than this. However, calculations using composite theory reveal that the larger aspect ratio of the clay versus glass fibers is not enough to explain all of the large differences in modulus reinforcement shown in Fig. 7. A significant part of the difference in modulus enhancement stems from the much higher modulus of MMT than glass fibers, i.e., 178 versus 72.4 GPa [58]. The comparison of MMT versus talc in a TPO matrix shown in Fig. 8 is more complex to explain, but similar factors are at play [103,117].

3.5. Nanocomposite thermal properties: dimensional stability

The high thermal expansion coefficients of neat plastics causes dimensional changes during molding and as the ambient temperature changes that are either undesirable or in some cases unacceptable for certain applications. The latter is a particular concern for automotive parts where plastics must be integrated with metals which have much lower coefficients of thermal expansion, CTE. Fillers are frequently added to plastics to reduce the CTE. For low aspect ratio filler particles, the reduction in CTE follows, more or less, a simple additive rule and is not very large; in these cases, the linear CTE changes are similar in all three coordinate directions. However, when high aspect ratio fillers, like fibers or platelets, are added and well oriented, the effects can be much larger; in these cases, the CTE in the three coordinate directions may be very different.

The fibers or platelets typically have a higher modulus and a lower CTE than the matrix polymer. As the temperature of the

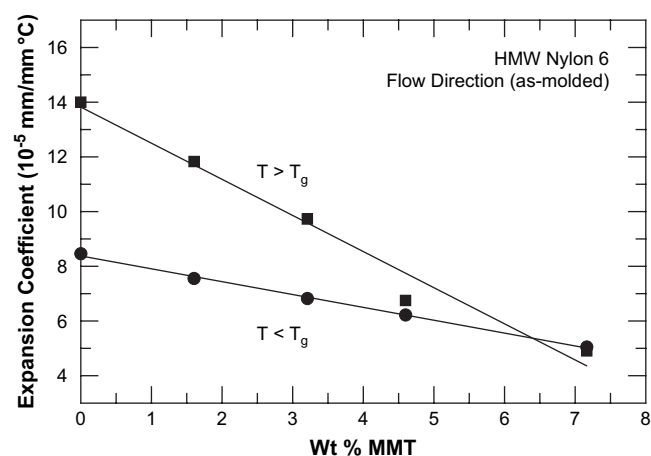


Fig. 11. Linear thermal expansion coefficients of as-molded nylon 6 nanocomposites determined in the flow direction for $T > T_g$ and $T < T_g$ [86]. Reproduced by permission of Elsevier Ltd.

composite changes, the matrix tries to extend or contract in its usual way; however, the fibers or platelets resist this change creating opposing stresses in the two phases. When the filler to matrix modulus is large, the restraint to dimensional change can be quite significant within the direction of alignment. Platelets can provide their restraint in two directions, when appropriately oriented, while fibers can only do so in one direction. Because of their shape differences, fibers can cause a greater reduction in the direction of their orientation than platelets can [166,170]. The CTE in the direction normal to the fibers or the platelet plane can actually increase when such fillers are added. Theories based on the mechanisms described above are available for quantitatively predicting CTE behavior [166,170].

Montmorillonite platelets are particularly effective for reducing CTE of plastics as shown in Fig. 11 for well-exfoliated nylon 6 nanocomposites [86]. These data were measured in the flow direction of injection molded bars. When the semicrystalline nylon 6 matrix is above its glass transition temperature, the CTE reduction is greater than when below the T_g . Of course, the neat nylon 6 has a higher CTE above T_g than below; however, because of its lower modulus above T_g , the MMT platelets are more effective for reducing CTE. Note that the two curves in Fig. 11 seem to cross at about 7 wt% MMT. For these specimens, the CTE in the transverse direction is also reduced by adding MMT but not quite as efficiently as in the flow direction since platelet orientation is not as great in the former as the latter direction. The CTE in the normal direction actually increases as MMT is added. These trends are quantitatively predicted by the theories mentioned earlier [86].

CTE behavior is also a major consideration for the TPO materials used in automotive applications [103,106,117]. As seen in Fig. 12, MMT is much more efficient at reducing CTE than talc in these materials [106]. Again, composite theories capture these trends reasonably well [117].

4. Variations and applications of polymer-based nanocomposites: properties other than reinforcement

Polymer composites comprising nanoparticles (including nanofibers where the fiber diameter is in the nanodimension range) are often investigated where reinforcement of the polymer matrix is achieved. While the reinforcement aspects are a major part of the nanocomposite investigations reported in the literature, many other variants and property enhancements are under active study and in some cases commercialization. The advantages of nanoscale particle incorporation can lead to a myriad of application

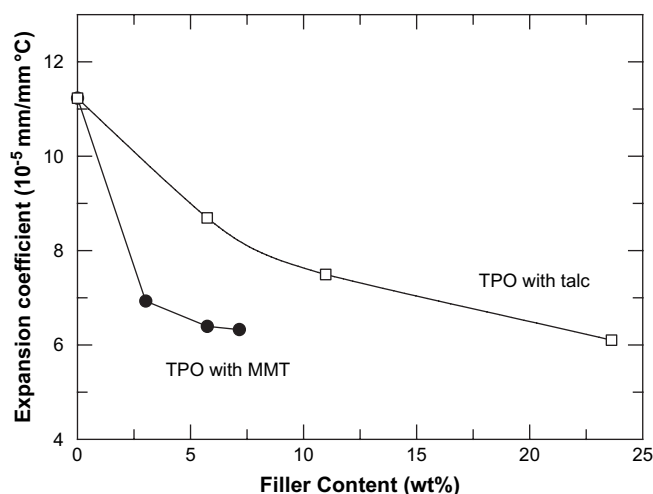
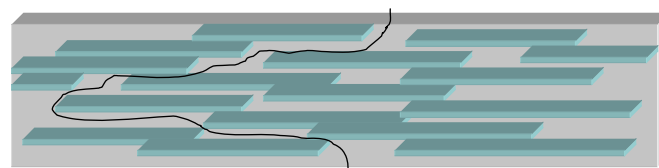


Fig. 12. Comparison of linear coefficients of thermal expansion (flow directions) as a function of filler content of TPO composites formed from MMT and talc [106]. Reproduced by permission of Elsevier Ltd.

possibilities where the analogous larger scale particle incorporation would not yield the sufficient property profile for utilization. These areas include barrier properties, membrane separation, UV screens, flammability resistance, polymer blend compatibilization, electrical conductivity, impact modification, and biomedical applications. Examples of nanoparticle, nanoplatelet and nanofiber incorporation into polymer matrices are listed in Table 2 along with potential utility where properties other than mechanical property reinforcement are relevant.

4.1. Barrier and membrane separation properties

The barrier properties of polymers can be significantly altered by inclusion of inorganic platelets with sufficient aspect ratio to alter the diffusion path of penetrant molecules as illustrated in Fig. 13. Various continuum models have been proposed to predict the permeability of platelet filled composites as listed in Table 3. These models are generally based on random, parallel platelets perpendicular to the permeation direction (random in only two directions). The model by Bharadwaj introduces an orientation factor [196]. At high aspect ratio which can be achieved (such as with exfoliated clay) in nanocomposites, significant decreases in permeability are predicted and observed in practice. Four of these models have been applied to polyisobutylene/vermiculite nanocomposites with aspect ratios predicted in the range of expectations [70]. The variability in the models was, however, shown to be



Permeation path imposed by nanoplatelet modification of polymer films

Fig. 13. Barrier to permeation imposed by nanoparticles imbedded in a polymeric matrix.

substantial. In many cases, the nanocomposites investigated can be approximated by the continuum models, thus the “nano-effect” is not observed. This should not be surprising as the dimensions of permeating gas molecules are still much lower than the nano-dimension modification. Differences would be expected in those cases where the T_g of the matrix polymer is changed. However, for practical applications the nanoscale dimensions are still quite important as transparency can be maintained along with surface smoothness for thin films; critical for food packaging applications.

Exfoliated clay modified poly(ethylene terephthalate) (PET) is one of the more prevalent nanocomposites investigated by both academic and industrial laboratories for barrier applications [197–199]. In situ polymerized PET-exfoliated clay composites were noted to show a 2-fold reduction in permeability with only 1 wt% clay versus the control PET [197]. PET-exfoliated clay composites also prepared via in situ polymerization using a clay-supported catalyst exhibited a 10 to 15-fold reduction in O_2 permeability with 1–5 wt% clay [198]. The moisture vapor transmission, however, did not show any significant change. Exfoliated clay modified chlorobutyl rubber showed decreased diffusion for several organic chemicals suggesting utility for chemical protective gloves/clothing [200]. Exfoliated clay added to polyamide 6/polyolefin (polyethylene or polypropylene) blends yielded an improved barrier to styrene permeation for melt blown films [201]. It was noted that the polymer blend nanocomposite was a better barrier than the control polyamide nanocomposite.

While most of the papers investigating barrier properties incorporate low levels of exfoliated clay, a novel approach employed producing a self-supporting clay fabric film followed by infiltration with an epoxy resin/amine hardener mixture and polymerization [202]. The resultant semitransparent nanocomposite film contained up to 77% volume fraction clay with an oxygen permeability 2–3 orders of magnitude lower than the control epoxy.

The concept of mixed matrix membranes involving molecular sieve inclusions in a polymer film to enhance the permselectivity properties for membrane separation was developed by Koros et al. [203] to address the limits imposed by upper bound limits typically observed with polymer membranes [204]. These inclusions (carbon molecular sieves, zeolite structures) need to be at nanolevel dimensions as the dense layer thickness of commercial membranes is in the range of 100 nm. This approach has shown promise in exceeding the noted upper bound in various studies [205,206]. The addition of silica nanoparticles to poorly packing polymer membranes (specifically poly(4-methyl-2-pentyne)) has been shown to yield even poorer packing and higher free volume [44]. This leads to increased permeability for larger organic molecules and a selectivity reversal for mixtures of these molecules with smaller molecules (e.g., *n*-butane/methane). This indicates that the separation process has changed from molecular sieving expected at low free volume and small void diameters to surface diffusion as the free volume and void diameters increase. The addition of nanoparticle TiO_2 to poly(trimethyl silylpropyne) (also a high free volume polymer with poor chain packing) showed a decrease in gas permeability up to 7 vol% TiO_2 with increasing permeability and higher free volume observed above 7 vol% loading [207].



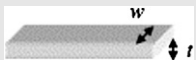
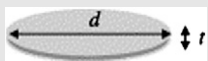
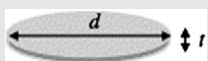
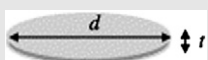
Table 2

Examples of nanoscale filler incorporated in polymer composites for property enhancement other than reinforcement

Nanofiller	Property enhancement(s)	Application/utility
Exfoliated clay	Flame resistance, barrier, compatibilizer for polymer blends	
SWCNT; MWCNT	Electrical conductivity, charge transport, Antimicrobial	Electrical/electronics/optoelectronics
Nanosilver	UV adsorption	UV screens
ZnO	Viscosity modification	Paint, adhesives
Silica	Charge transport	Photovoltaic cells
CdSe, CdTe	Electrical conductivity, barrier, charge transport	Electrical/electronic
Graphene	Improved stability, flammability resistance	Sensors, LEDs
POSS		

Table 3

Models for predicting barrier properties of platelet filled nanocomposites (adapted from Ref. [70], copyright by Elsevier)

Model	Filler type	Particle geometry	Formulas	Reference
Nielsen	Ribbon ^a		$(P_0/P)(1 - \phi) = 1 + \alpha\phi/2$	[192]
Cussler (Regular array)	Ribbon ^a		$(P_0/P)(1 - \phi) = 1 + (\alpha\phi)^2/4$	[193]
(Random array)	Ribbon ^a		$(P_0/P)(1 - \phi) = (1 + \alpha\phi/3)^2$	[193]
Gusev and Lusti	Disk ^b		$(P_0/P)(1 - \phi) = \exp[(\alpha\phi/3.47)^{0.71}]$	[194]
Fredrickson and Bicerano	Disk ^b		$(P_0/P)(1 - \phi) = 4(1 + x + 0.1245x^2)/(2 + x)^2$ where $x = \alpha\phi/2 \ln(\alpha/2)$	[195]
Bharadwaj	Disk ^b		$(P_0/P)(1 - \phi) = 1 + 0.667\alpha\phi(S + (1/2))$ where S = orientation factor (from $-1/2$ to 1)	[196]

^a For ribbons, length is infinite, width, w ; thickness, t ; aspect ratio, $\alpha \equiv w/t$.^b For disks, circular shape of diameter d and thickness t ; aspect ratio, $\alpha \equiv d/t$.

4.2. Flammability resistance

Increased flammability resistance has been noted as an important property enhancement involving nanoplatelet/nanofiber modification of polymeric matrices. While the specific reasons for this are under continuing investigation, a qualitative explanation observed in many studies involves the formation of a stable carbon/nanoplatelet or nanofiber surface. This surface exhibits analogous characteristics to intumescent coatings whereby the resultant “char” provides protection to the interior of the specimen by preventing continual surface regeneration of available fuel to continue the combustion process. The primary advantage noted with nanofiller incorporation is the reduction in the maximum heat release rate (determined by cone calorimetry) [137,208]. While significant reductions can be observed in the maximum heat release rates, the total heat release remains constant with nanofiller addition. The relevance of reducing the maximum heat release rate is to minimize the flame propagation to adjacent areas in the range of the ignited material (dimension range of meter(s)). The flammability improvements for nanofiller addition are less advantageous when the more common empirical regulatory (pass/fail) flammability tests are conducted (UL94, ASTM flammability tests) [137,208,209]. In specific cases, the nanoparticle addition can result in reduced flammability rating due to the melt viscosity increase preventing dripping as a mechanism of flame extinguishment (e.g., change UL94 rating from V-2 to HB) [209]. The primary advantage for nanofiller addition for these tests generally involves reduction in the flame retardant additives that need to be incorporated to pass the specific test [137,209,210]. This has been observed in various nanoparticle modified composites including exfoliated clay with halogen-based flame retardants/Sb₂O₃ [211] and EVA (ethylene-vinyl acetate copolymer) nanocomposites with magnesium hydroxide nanoparticles and microcapsulated red phosphorus [212].

The majority of the flame retardant studies on nanofiller incorporation in polymers involves exfoliated clay. Studies involving polyamide 6 [213,214] and polypropylene [215] yielded similar observations with reduced peak heat release rate but no change in the total heat release with exfoliated clay addition. This is illustrated in Fig. 14 for a generalized data for nanofiller modified polymers. While the curve position and shape will vary for different polymer matrix materials and nanofiller incorporation, the generalized behavior of decreased peak heat release rate with basically no change in the overall heat release (area under the curve) is very typical. The surface characteristics during and after forced combustion show that incomplete surface coverage will lead to poorer flammability resistance and can be related to low nanofiller level,

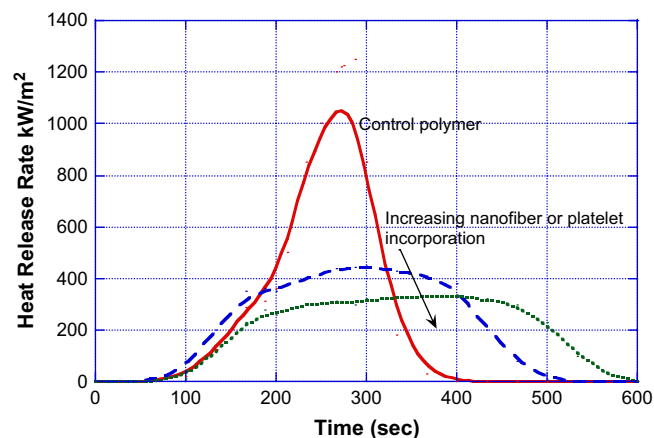


Fig. 14. Generalized behavior for nanofiber or platelet modified polymers in the cone calorimetry heat release rate test.

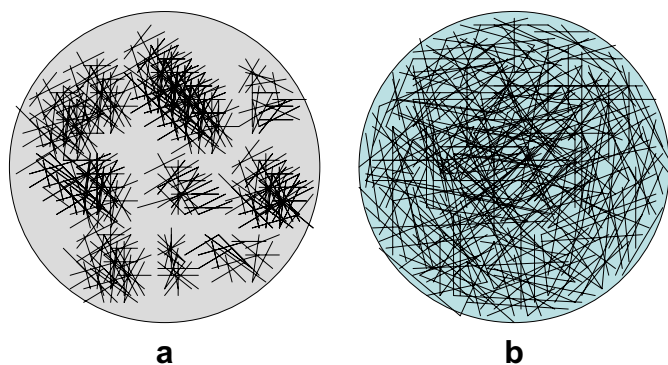


Fig. 15. Surface structure of nanocomposites during/after forced combustion: (a) incomplete surface coverage due to low nanofiber level, agglomeration during combustion and/or low aspect ratio; (b) desired surface dispersion during/after forced combustion.

low aspect ratio, poor dispersion and/or agglomeration during combustion. This generalized behavior, illustrated in Fig. 15, is true for exfoliated clay as well as carbon nanotubes as discussed below.

Studies involving carbon nanotubes have also shown the decrease in the peak heat release rate with no change in the total heat release [216,217] with effectiveness equal to or better than exfoliated clay. The level of dispersion of the carbon nanotubes in the polymer matrix was shown to be an important variable [216]. Upon combustion, the surface layer was enriched with a protective nanotube network providing a thermal and structural barrier to the combustion process. Continuity of the network (as illustrated in Fig. 15) was important to achieve optimum performance as very low levels of nanotube incorporation or poor dispersion did not allow a continuous surface network during the combustion process. It is noted that the incorporation of nanoclay and carbon nanotubes often results in slightly earlier ignition than the unmodified polymer presumably due to the increased thermal conductivity. However, at the later stages of combustion, the reinforcement of the char layer provides a stable thermal barrier preventing regeneration of polymer at the surface available for rapid combustion.

4.3. Polymer blend compatibilization

A primary mechanism in compatibilization of phase separated polymer blends involves lowering the interfacial tension between the phases and preventing coalescence of the particles during melt processing. This can be achieved by addition of graft or block

copolymers with constituents equal to or compatible with the blend components. It has been observed in many cases that the addition of nanoparticles (particularly exfoliated clay) can also prevent the coalescence retaining improved dispersion after shear mixing. Specific examples involving exfoliated clay compatibilization include polycarbonate/poly(methyl methacrylate) [218], poly(2,6-dimethyl-1,4-phenylene oxide)/polyamide 6 [219], polyamide 6/ethylene–propylene rubber [220], polystyrene/poly(methyl methacrylate) [221] and poly(vinylidene fluoride)/polyamide 6 blends [222]. An example of exfoliated clay compatibilization of a poly(methyl methacrylate)/polystyrene (70/30 by weight) blend is illustrated in Fig. 16 [221]. After shearing and annealing above the blend component T_g s, the blend containing exfoliated clay shows the ability to resist coalescence. Nanoscale SiO_2 particle compatibilization was noted for polystyrene/polypropylene blends where a significant reduction in the polystyrene phase dimensions was observed [223]. The compatibilization was hypothesized to be due to increased viscosity retarding coalescence.

Several additional hypotheses have been noted in the literature. One explanation is that the nanoparticles concentrate at the interface preventing coalescence by a barrier-type mechanism. Another hypothesis notes that both polymers bound by physical [224] or chemical interactions [221] on the nanoparticle will concentrate at the interface similar to a block or graft copolymer comprising both components of the blend. In the case of physical interactions, it was noted that for a polypropylene/polystyrene blend both polymers were intercalated into the clay gallery with the polymer chain extending outside the particle [224]. The nanoparticle size is important for both explanations and offers an advantageous property not achievable at higher length scales.

4.4. Biomedical applications

The applicability of polymer nanotechnology and nanocomposites to emerging biomedical/biotechnological applications is a rapidly emerging area of development of which this discussion can only briefly cover. One area of intense research involves electrospinning for producing bioresorbable nanofiber scaffolds for tissue engineering applications. This might be construed as a nanocomposite as the resultant scaffold allows for cell growth yielding a unique composite system. Another area also involving nanofibers is the utilization of electrically conducting nanofibers based on conjugated polymers for regeneration of nerve growth in a biological living system.

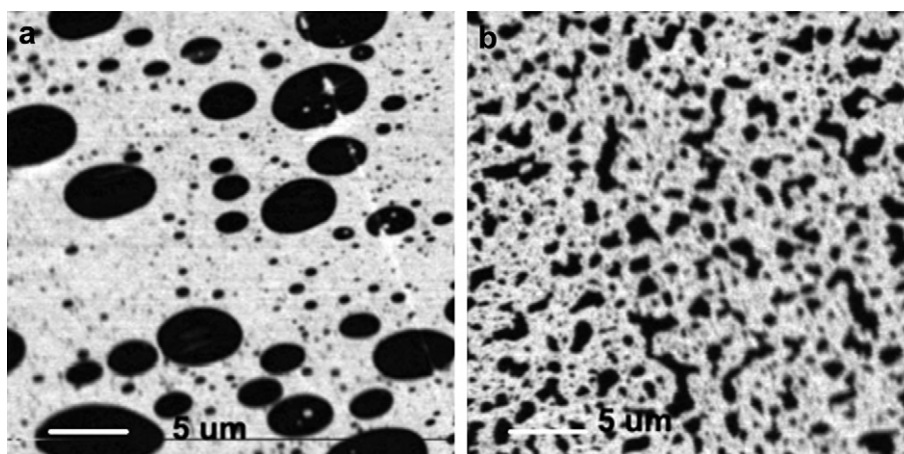


Fig. 16. Scanning transmission X-ray microscopic images ($30\ \mu\text{m} \times 30\ \mu\text{m}$) of PS/PMMA blends annealed at $190\ ^\circ\text{C}$ for 14 h (taken at 285.2 eV, the adsorption energy of PS, PS is dark): (a) PS/PMMA (30/70), (b) PS/PMMA/Closite 6A (27/63/10). Reproduced with permission of Ref. [221], copyright (2006) American Chemical Society.

Nanoparticle silver, silver oxide and silver salts have been incorporated into polymer matrices to provide antimicrobial/biocidal activity [225–227]. Nanoscale silver was shown to be a much better antimicrobial additive to nylon 6 than microscale silver particles [227] due to the much higher rate of silver ion release. Nanosilver (5–50 nm) at levels of 0.1–1.0 wt% in poly(methyl methacrylate) bone cement exhibited high antibacterial activity for joint arthroplasty utility [228] without the cytotoxicity of silver salts.

Polymer nanocomposites based on hydroxyapatite ($\text{Ca}_{10}(\text{PO}_4)_6(\text{OH})_2$) have been investigated for bone repair and implantation [229]. Hydroxyapatite, a major constituent of hard tissue, exhibits undesirable mechanical properties if directly employed thus polymer-based matrix composites are desired. Biodegradation of the matrix is also desired to allow infiltration of new bone growth at the repair site. Often natural polymers (polysaccharides, polypeptides, collagen, chitosan) or synthetic biodegradable polymers are employed as the matrix in these studies. Collagen derived gelatin [230] and poly-2-hydroxyethyl-methacrylate/poly(ϵ -caprolactone) [231] nanocomposites based on hydroxyapatite are examples of systems studied for bone repair systems.

Electrospinning of biodegradable polymer solutions is a popular method to produce nanofiber scaffolds for tissue engineering applications. Poly(L-lactic acid)/exfoliated montmorillonite clay/salt solutions were electrospun followed by salt leaching/gas foaming [232]. The resultant scaffold structure contained both nano- and micro-sized pores offering a combination of cell growth and blood vessel invasion micro-dimensions along with nanodimensions for nutrient and metabolic waste transport.

Polymer matrix nanocomposites have been proposed for drug delivery/release applications. The addition of nanoparticles can provide an impediment to drug release allowing slower and more controlled release, and reduced swelling [233] and improved mechanical integrity [234] of hydrogel-based nanocomposites. Iron oxide nanoparticles have been investigated for various applications including drug delivery, magnetic resonance imaging contrast enhancement, immunoassay and cellular therapy. These investigations often employ magnetite (Fe_3O_4) dispersed in a polymeric microsphere or microcapsule involving biodegradable and/or natural polymers [235,236]. Poly(L-lysine) microspheres containing magnetic nanoparticles prepared by coacervation were prepared and characterized for potential use in targeted drug delivery applications [237]. Iron and cobalt nanoparticles encapsulated in polydimethylsiloxane have been noted for treating retinal detachment disorders [238,239]. A novel imprint lithography method based on a crosslinked perfluoroether templating mold has been employed to fabricate uniform micro- and nanoparticles from organic polymers including biodegradable polymers such as poly(lactic acid) [240]. Inclusion of inorganic nanoparticles such as discussed above has potential for a diverse range of biomedical applications using this method.

4.5. Fuel cell applications

Fuel cell applications involve polymers in the proton exchange membrane, binder for the electrodes and matrix for bipolar plates. The electrodes typically comprise carbon black particles (0.5–1.0 μm) with Pt catalyst particles of 2–5 nm and a polymeric binder (usually Nafion[®]). Platinum nanoparticles deposited onto single-walled carbon nanotubes with Nafion[®] as a binder were shown to give improved performance over the conventional carbon black-based electrodes [241]. Nanoparticle incorporation in the proton exchange membrane has been noted in numerous publications to improve mechanical properties as well as to enhance proton conductivity. Additionally with direct methanol fuel cells,

nanoparticles have been incorporated to reduce methanol crossover [242].

Heteropolyacids (HPA) (e.g., $\text{H}_3\text{PW}_{12}\text{O}_{40}$; $\text{H}_3\text{PMo}_{12}\text{O}_{40}$) have been added to proton exchange membranes to yield improved proton conductivity at higher temperatures while retaining good mechanical properties [243–246]. The particle size of the HPA inclusions was generally in the nanorange. Silica nanoparticle inclusion in proton exchange membranes gave lower methanol crossover in several studies [247,248]. Zirconium phosphate [249], zirconium hydrogen phosphate [250] and TiO_2 [251] nanoparticle incorporation in proton exchange membranes exhibited promise in direct methanol fuel cells. Nanoclay modified Nafion[®] (Iapointe [252] and montmorillonite [253]) membranes have been reported to offer improvements over the unmodified controls. Sulfonated carbon nanofibers incorporated into a sulfonated EPDM proton exchange membrane yielded an order of magnitude improvement in the proton conductivity achieving performance comparable to the state-of-the-art Nafion[®] 117 [254].

4.6. Electrical/electronics, optoelectronics, and sensors

Nanotechnology is deeply embedded in the design of advanced devices for electronic and optoelectronic applications. The dimensional scale for electronic devices has now entered the nanorange. The utility of polymer-based nanocomposites in these areas is quite diverse involving many potential applications as well as types of nanocomposites. One specific nanocomposite type receiving considerable interest involves conjugated polymers and carbon nanotubes. A recent review of this area notes a litany of potential applications including photovoltaic (PV) cells and photodiodes, supercapacitors, sensors, printable conductors, light emitting diodes (LEDs) and field effect transistors [255]. This paper can only briefly discuss the nanocomposite technology applied to this broad field.

The electrical conductivity of carbon nanotubes in insulating polymers has also been a topic of considerable interest. The potential applications include electromagnetic interference shielding, transparent conductive coatings, electrostatic dissipation, supercapacitors, electromechanical actuators and various electrode applications [256,257]. The percolation threshold for electrical conductivity of epoxy composites containing multi-wall carbon nanotubes was found to be 0.0025 wt% MWCNT [258] considerably lower than nanoscale dispersed carbon black particles. The threshold conductivity of single-walled carbon nanotubes in epoxy composites was noted to be a function of the SWCNT type with values as low as 0.00005 vol fraction [259]. Water dispersed carbon black particles (42 nm) added to acrylic emulsions yielded electrical conductivity percolation levels as low as 1.5 vol% in dried films [260]. In this system, the carbon black particles concentrate at the interface between the emulsion particles during drying yielding a percolation network. The modulus of the emulsion system chosen as the matrix was noted to be an important variable with higher modulus (higher T_g) yielding lower threshold percolation values.

The basic device structure for organic/polymeric PV and LED devices is shown in Fig. 17. The major difference between the two

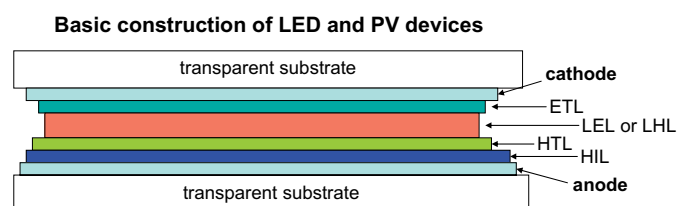


Fig. 17. Generalized diagram of LED and PV device construction.

devices is the light emitting layer and the light harvesting layer. While all the potential layers are noted, actual devices often do not contain all the layers. Polymer-based nanocomposites are most relevant for the anode, hole injection layer, light emitting layer and light harvesting layer. In the case where flexible transparent substrates are desired, nanocomposite or nanolayered combinations of polymer and barrier nanomaterials can be employed to provide barrier properties to oxygen and water permeation.

Silicon-based photovoltaic (PV) devices offer high efficiency, excellent stability and proven commercial utility. Organic/polymer-based PV devices offer the potential for lower cost and more flexible manufacture but need significant improvements in both efficiency and long term stability. Conjugated polymers are often employed in the organic-based device light harvesting layer but have limitations in charge transport. Combinations of conjugated polymer with inorganic semiconductors have been proposed as a resolution to this deficiency. Cadmium–selenium, CdSe, nanorod incorporation in poly(3-hexylthiophene) yielded power conversion efficiency of 1.7% [261]. Silicon solar cells, however, typically deliver power conversion efficiencies of 10% or greater. Layer-by-layer assembly of functionalized poly(phenylene vinylene) and CdSe nanoparticle composites yielded uniform thin films with a power conversion efficiency of 0.71% [262]. A functionalized polystyrene containing an electroactive carbazole pendant group and an amine salt pendant group capable of electrostatic interaction with CdTe was described for potential PV applications [263]. Poly(3-hexylthiophene)–ZnO nanofiber composites exhibited a power conversion efficiency of 0.53% noted to be significantly better than the analogous bilayer structure of the noted components [264]. Spherical ZnO nanoparticle (20–40 nm) incorporation into poly(3-hexylthiophene) was ineffective at low levels of incorporation (20–30 wt%) but large improvements were observed at 50–60 wt% addition yielding a power conversion efficiency increase of 35 times to a value of 0.42% [265]. SWCNT incorporation into poly(3-octylthiophene) increased the short circuit current by two orders of magnitude and improved the important fill factor [266]. Ink jet printing is a potential method for producing low cost, high volume PV and LED devices. The ink jet printing of the nanocomposite of poly(vinyl alcohol) and CdTe for these devices was demonstrated by Tekin et al. [267].

The primary material presently employed for the hole injection layer (HIL) is PEDOT:PSS (poly(3,4-ethylene dioxythiophene):poly(styrene sulfonic acid)) but has limitations in life-time performance. The addition of silver nanoparticles (3–6 nm) to PEDOT:PSS resulted in maximum device luminance at 20 wt% [268]. The addition of nickel nanoparticles (30 nm) into the PEDOT:PSS HIL was

also shown to improve device performance attributed to the improved hole current [269]. Gold nanoparticle (5–10 nm) incorporation into poly(9,9'-dioctylfluorene) (LEL layer) gave higher external quantum efficiencies and improved oxygen stability compared to the unmodified polyfluorene [270,271]. Poly(9,9'-dioctylfluorene)-layered silicate nanocomposites were also demonstrated to improve device stability as well as offering higher quantum efficiencies over the unmodified polyfluorene [272]. Poly(phenylene) with polyhedral oligomeric silsesquioxane (POSS) side groups inhibited interchain interaction leading to improved fluorescence quantum yields in solution and photoluminescent thermal stability in bulk [273].

Exfoliated graphite sheets (graphene) have been only recently investigated in nanocomposites [274] at least partly due to the lack of methods to achieve high levels of exfoliation [275,276]. It was noted that the electrical conductivity for polystyrene–graphene nanocomposites had a percolation threshold of 0.1 vol% rivaling carbon nanotubes [274]. The electrical conductivity at 1 vol% was 0.1 S/cm. The emerging interest of graphene in electronics applications parallels that which occurred with carbon nanotube discovery. Graphene, in sheet form, may offer promise in replacing silicon as Moore's law limits are achieved [277].

Conjugated polymers with various nanoscale filler inclusions have been investigated for sensor applications including gas sensors, biosensors and chemical sensors. The nanofillers employed include metal oxide nanowires, carbon nanotubes, nanoscale gold, silver, nickel, copper, platinum and palladium particles [278]. With carbon nanotubes, the electrical resistance was found to be significantly changed by exposure to specific gases such as NO₂ and NH₃ [279]. A nanocomposite of SWCNT/polypyrrole yielded a gas sensor sensitivity similar to SWCNT alone [280]. The sensing capability of these nanocomposites can be based on conductivity changes due to gas or chemical interactions with either the nanofiller or the conjugated polymer, pH changes, electrochromic or electro-optical property changes, catalytic activity, chemiluminescent property or biological recognition. Examples of sensors for dopamine detection include a poly(anilineboronic acid)/carbon nanotube composite [281] and a polyaniline/gold composite hollow sphere system [282]. A review of conjugated polymer nanocomposites employed as sensors has been recently published [278].

5. Commercial applications of polymer-based nanocomposites

A question often posed is “with all the interest and associated large R&D expenditures in nanotechnology (including polymer

Table 4
Examples of nanocomposite commercial utility

Polymer matrix	Nanoparticle	Property improvement	Application	Company and/or product trade name
Polyamide 6	Exfoliated clay	Stiffness	Timing belt cover: automotive	Toyota/Ube
TPO (thermoplastic polyolefin)	Exfoliated clay	Stiffness/strength	Exterior step assist	General Motors
Epoxy	Carbon nanotubes	Strength/stiffness	Tennis rackets	Babolat
Epoxy	Carbon nanotubes	Strength/stiffness	Hockey sticks	Montreal: Nitro Hybtonite®
Polyisobutylene	Exfoliated clay	Permeability barrier	Tennis balls, tires, soccer balls	InMat LLC
SBR, natural rubber, polybutadiene	Carbon black (20–100 nm: primary particles)	Strength, wear and abrasion	Tires	Various
Various	MWCNT	Electrical conductivity	Electrostatic dissipation	Hyperion
Unknown	Silver	Antimicrobial	Wound care/bandage	Curad®
Nylon MXD6, PP	Exfoliated clay	Barrier	Beverage containers, film	Imperm™: Nanocor
SBR rubber	Not disclosed	Improved tire performance in winter	Winter tires	Pirelli
Natural rubber	Silver	Antimicrobial	Latex gloves	
Various	Silica	Viscosity control, thixotropic agent	Various	
Polyamides nylon 6, 66, 12	Exfoliated clay	Barrier	Auto fuel systems	Ube

Information from company web pages and industry journal reviews.

nanocomposites) why is there not more commercial impact?" Often major discoveries take several decades to reach large commercial impact (polyethylene, carbon fiber composites as examples) as the cost/performance variables upon discovery are outside the realm of commodity utility and additional advances are required to achieve an economically competitive position. The commodities of today were the specialties of the past and even the automobile was a specialized article of commerce for several decades. Such is the case with the technologies being developed with polymer-based nanocomposites. While many of the applications being commercialized today will remain specialties, there are areas where the specialty polymer nanocomposites of today will be the commodities of the future. Examples of commercial polymer based nanocomposites are listed in Table 4.

The most publicized application for polymer nanocomposites was an automotive application by Toyota for a timing belt cover. The utilization of exfoliated clay reinforcement of TPO (thermoplastic polyolefin) came later utilized by General Motors for an exterior step assist for another automotive application. Obviously, there are many more applications involving exfoliated clay reinforcement, however, many of these have not been publicized such as those noted above.

One of the initial uses for exfoliated clay in barrier applications involved a 20 μm coating on the interior of a tennis ball to prevent depressurization. The product was developed by InMat LLC and introduced in 2001. Sports equipment was one of the initial areas where carbon fiber composites were commercialized. This is also true for carbon nanotubes where the carbon nanotubes (at low levels) reinforce the epoxy matrix of the carbon fiber composite in specialty tennis rackets and hockey sticks. In such applications, performance overrides the economic disadvantages of the expensive carbon nanotube inclusion.

6. Comments on the future of polymer matrix based nanocomposites

An area where nanocomposites could achieve a dramatic commercial prominence is in advanced composites. Carbon fiber reinforced composites have a limit on the achievable properties (particularly in cross-ply composites) due to the low modulus and strength of the matrix phase. Modification of the matrix phase with carbon nanotubes at the lower scale of dimensions and carbon nanofibers at a higher dimensional scale would allow for significant increases in the modulus and strength contributions of the matrix to the overall composite properties. While this would offer some improvement in unidirectional composites, it could be dramatic in the case of cross-ply composites which are the major type of composite structure utilized in advanced composite applications. This concept is under present consideration and could allow a step change in the advanced composite field. The basic concept has already been commercially employed in specialty sports equipment (tennis rackets and hockey sticks). These improvements are key to future aircraft and wind energy turbine applications. This approach is analogous to naturally occurring composite structures where the hierarchical construction method employs several dimensional scales beginning at the nanolevel. The same concept is also relevant to the more commodity reinforced composites where exfoliated clay could be added to the matrix for unsaturated polyester-fiberglass composites or other fiberglass reinforced matrix polymers.

As the secrets of nature's methodology to optimize material properties by nanolevel construction are unlocked (biomimetics), translation of these findings to polymer nanocomposites should allow for further advances. Nanostructured surfaces have been noted to yield superhydrophobic character (lotus leaf) and exceptional adhesion (gecko foot). The confluence of the biological and polymer material science disciplines often involves the design of

nanoscale polymeric blends and composite systems to mimic the biological systems.

Carbon nanotube or exfoliated graphite (graphene) offers substantial opportunities in the electrical/electronics/optoelectronics areas as well as potential in specific emerging technologies. One specific area would be replacement of ITO as a transparent conductor for lower cost and flexible devices. Carbon nanotube sheets have been proposed [283] and the potential for carbon nanotube-conjugated polymer composites would be of interest if sufficient electrical conductivity can be obtained ($>10^3 \text{ S/cm}$). The potential of low cost graphene production is yet to be realized and large scale utility will be awaiting the synthetic breakthrough.

An additional area not discussed in detail in this review involves the importance of morphology control which includes both dispersion and alignment. These issues have been discussed in many of the papers already cited in this review as well as in recent reviews [156,284]. Obtaining the optimum properties for nanocomposites will usually require excellent dispersion of the nanoparticles. The tendency for nanoparticles (including platelets and fibers of nanoscale dimensions) to coalesce into macroscale agglomerates can seriously impact the achievable properties. In specific cases, excellent isotropic dispersion may not be the desired morphology but rather a hierarchical morphology that offers unique properties such as those observed with percolation pathways to maximize electrical conductivity or patterned morphology to achieve novel optical or electronic properties [284].

References

- [1] Mark JE, Jiang CY, Tang MY. *Macromolecules* 1984;17:2613–6.
- [2] Wilkes GL, Orler B, Huang H. *Polym Prep* 1985;26:300–1.
- [3] Wen J, Wilkes GL. *Chem Mater* 1996;8:1667–81.
- [4] Kojima Y, Usuki A, Kawasumi M, Okada A, Kurauchi T, Kamigaito O. *J Polym Sci Part A Polym Chem* 1993;31:983–6.
- [5] Okada A, Fukushima Y, Kawasumi M, Inagaki S, Usuki A, Sugiyama S, et al. *US Patent* 4,739,007; 1988.
- [6] Kawasumi M. *J Polym Sci Part A Polym Chem* 2004;42:819–24.
- [7] Loo YL, Register RA, Ryan AJ. *Phys Rev Lett* 2000;84:4120–3.
- [8] Loo YL, Register RA, Ryan AJ. *Macromolecules* 2002;35:2365–74.
- [9] Santana OO, Müller AJ. *Polym Bull* 1994;32:471–7.
- [10] Woo E, Huh J, Jeong YG, Shin K. *Phys Rev Lett* 2007;98:136103.
- [11] Shin K, Woo E, Jeong YG, Kim C, Huh J, Kim KW. *Macromolecules* 2007;40:6617–23.
- [12] Wu H, Wang W, Yang H, Su Z. *Macromolecules* 2007;40:4244–9.
- [13] Di Maio E, Iannace S, Sorrentio L, Nicolais L. *Polymer* 2004;45:8893–900.
- [14] Zhang QX, Yu ZZ, Yang M, Ma J, Mai YW. *J Polym Sci Part B Polym Phys* 2003;41:2861–9.
- [15] Mu B, Wang Q, Wang H, Jian L. *J Macromol Sci Part B Phys* 2007;46:1093–104.
- [16] Nam JY, Ray SS, Okamoto M. *Macromolecules* 2003;36:7126–31.
- [17] Lincoln DM, Vaia RA, Krishnamoorti R. *Macromolecules* 2004;37:4554–61.
- [18] Li L, Li CY, Ni C, Rong L, Hsiao B. *Polymer* 2007;48:3452–60.
- [19] Phang IY, Pramoda KP, Liu T, He C. *Polym Int* 2004;53:1282–9.
- [20] Wu D, Zhou C, Fan X, Mao D, Bian Z. *Polym Polym Compos* 2005;13:61–71.
- [21] Bilotti E, Fischer HR, Peijs T. *J Appl Polym Sci* 2008;107:1116–23.
- [22] Xu D, Wang Z. *Polymer* 2008;49:330–8.
- [23] Homminga D, Goderis B, Dolbnya I, Reynaers H, Groeninckx G. *Polymer* 2005;46:11359–65.
- [24] Chen EC, Wu TM. *J Polym Sci Part B Polym Phys* 2008;46:158–69.
- [25] Kim B, Lee SH, Lee D, Ha B, Park J, Char K. *Ind Eng Chem Res* 2004;43:6082–9.
- [26] Harrats C, Groeninckx G. *Macromol Rapid Commun* 2008;29:14–26.
- [27] Guérin G, Prud'homme RE. *J Polym Sci Part B Polym Phys* 2007;45:10–7.
- [28] Rittigstein P, Torkelson JM. *J Polym Sci Part B Polym Phys* 2006;44:2935–43.
- [29] Pluta M, Jeszka JK, Boiteux G. *Eur Polym J* 2007;43:2819–35.
- [30] Lee KJ, Lee DK, Kim YW, Choe WS, Kim JH. *J Polym Sci Part B Polym Phys* 2007;45:2232–8.
- [31] Xu H, Yang B, Wang J, Guang S, Li C. *J Polym Sci Part A Polym Chem* 2007;45:5308–17.
- [32] Ramasundaram SP, Kim KJ. *Macromol Symp* 2007;249–250:295–302.
- [33] Huang JC, He CB, Xiao Y, Mya KY, Dai J, Siow YP. *Polymer* 2003;44:4491–9.
- [34] Pham JQ, Mitchell CA, Bahr JL, Tour JM, Krishnamoorti R, Green PF. *J Polym Sci Part B Polym Phys* 2003;41:3339–45.
- [35] Böhning M, Goering H, Hao N, Mach R, Oleszak F, Schönhals A. *Rev Adv Mater Sci* 2003;5:155–9.
- [36] Xu W, Ge M, Pan WP. *J Therm Anal Calorim* 2004;78:91–9.

- [37] Fragiadakis D, Pissis P. *J Non-Cryst Solids* 2007;353:4344–52.
- [38] Shi X, Gan Z. *Eur Polym J* 2007;43:4852–8.
- [39] Huskić M, Žigon M. *Eur Polym J* 2007;43:4891–7.
- [40] Yuen SM, Ma CCM, Lin YY, Kuan HC. *Compos Sci Technol* 2007;67:2564–73.
- [41] Uthirakumar P, Nahm KS, Hahn YB, Lee YS. *Eur Polym J* 2004;40:2437–44.
- [42] Sun Y, Luo Y, Jia D. *J Appl Polym Sci* 2008;107:2786–92.
- [43] Chang JH, Mun MK, Kim JC. *J Appl Polym Sci* 2007;106:1248–55.
- [44] Merkel TC, Freeman BD, Spontak RJ, He Z, Pinnau I, Meakin P, et al. *Science* 2002;296:519–22.
- [45] Kim JH, Koros WJ, Paul DR. *Polymer* 2006;47:3094–103 and 3104–3111.
- [46] Huang Y, Paul DR. *J Polym Sci Part B Polym Phys* 2007;45:1390–8.
- [47] Van Olphen H. *An introduction to clay colloid chemistry*. New York: Interscience; 1963.
- [48] LeBaron PC, Wang Z, Pinnavaia TJ. *Appl Clay Sci* 1999;15:11–29.
- [49] Pinnavaia TJ, Beall GW, editors. *Polymer–clay nanocomposites*. New York: John Wiley & Sons; 2000.
- [50] Yaviv S, Cross H, editors. *Organo-clay complexes and interactions*. New York: Marcel Dekker; 2002.
- [51] Ray SS, Okamoto M. *Prog Polym Sci* 2003;28:1539–641.
- [52] Mai Y, Yu Z, editors. *Polymer nanocomposites*. Cambridge: Woodhead; 2006.
- [53] Hussain F, Hojjati M. *J Compos Mater* 2006;40(17):1511–65.
- [54] Hunter DL, Kamena KW, Paul DR. *MRS Bull* 2007;32:2806.
- [55] Xie W, Gao Z, Liu K, Pan W-P, Vaia R, Hunter D, et al. *Thermochim Acta* 2001;367–368:339–50.
- [56] Xie W, Gao Z, Pan W-P, Hunter D, Singh A, Vaia R. *Chem Mater* 2001;13:2979–90.
- [57] Xie W, Xie R, Pan W-P, Hunter D, Koene B, Tan L-S, et al. *Chem Mater* 2002;14:4837–45.
- [58] Fornes TD, Paul DR. *Polymer* 2003;44:4993.
- [59] Paul DR, Zeng QH, Yu AB, Lu GQ. *J Colloid Interface Sci* 2005;292:462.
- [60] Heinz H, Vaia RA, Krishnamoorti R, Farmer BL. *Chem Mater* 2007;19:59–68.
- [61] Ploehn HJ, Liu C. *Ind Eng Chem Res* 2006;45:7025–34.
- [62] Fukushima Y, Inagaki S. *J Inclusion Phenom* 1987;5:473–82.
- [63] Kojima Y, Usuki A, Kawasumi M, Okada A, Kurauchi T, Kamigaito O. *J Polym Sci Part A Polym Chem* 1993;31:1755–8.
- [64] Biasci L, Aglietto M, Ruggeri G, Ciardelli F. *Polymer* 1994;35(15):3296–309.
- [65] Huang X, Lewis S, Brittann WJ. *Macromolecules* 2000;33:2000–4.
- [66] Zhou Q, Fan X, Xia C, Mays J, Advincula R. *Chem Mater* 2001;13:2465–7.
- [67] Albrecht M, Ehrler S, Mühlebach A. *Macromol Rapid Commun* 2003;24:382–7.
- [68] Kiersnowski A, Piglowski J. *Eur Polym J* 2004;40:1199–207.
- [69] Goldberg HA, Feeney CA, Karim DP, Farrell M. *Rubber World* 2002;226:1–17. see also p. 20 and 37.
- [70] Takahashi S, Goldberg HA, Feeney CA, Karim DP, Farrell M, O'Leary K, et al. *Polymer* 2006;47:3083–93.
- [71] Vaia RA, Ishii H, Giannelis EP. *Chem Mater* 1993;5:1694.
- [72] Vaia RA, Teukolsky RK, Giannelis EP. *Chem Mater* 1994;6:1017–22.
- [73] Vaia RA, Jandt KD, Kramer EJ, Giannelis EP. *Macromolecules* 1995;28:8080–5.
- [74] Giannelis EJ. *Adv Mater* 1996;8(1):29.
- [75] Vaia RA, Jandt KD, Kramer EJ, Giannelis EP. *Chem Mater* 1996;8:2628–35.
- [76] Vaia RA, Giannelis EP. *Macromolecules* 1997;30:7990–9.
- [77] Vaia RA, Giannelis EP. *Macromolecules* 1997;30:8000–9.
- [78] Lee JY, Baljon ARC, Lorin RF. *J Chem Phys* 1990;111(21):9754–60.
- [79] Manias E, Chen H, Krishnamoorti R, Genzer J, Kramer EJ, Giannelis EP. *Macromolecules* 2000;33:7955–66.
- [80] Anastasiadis SH, Karatasos K, Vlachos G. *Phys Rev Lett* 2000;84(5):915–8.
- [81] Vaia RA, Giannelis EP. *Polymer* 2001;42:1281–5.
- [82] Cho JW, Paul DR. *Polymer* 2001;42:1083.
- [83] Dennis HR, Hunter DL, Chang D, Kim S, White JL, Cho JW, et al. *Polymer* 2001;42:9513.
- [84] Fornes TD, Yoon PJ, Keskkula H, Paul DR. *Polymer* 2001;42:9929.
- [85] Fornes TD, Yoon PJ, Hunter DL, Keskkula H, Paul DR. *Polymer* 2002;43:5915.
- [86] Yoon PJ, Fornes TD, Paul DR. *Polymer* 2002;43:6727.
- [87] Fornes TD, Paul DR. *Polymer* 2003;44:3945.
- [88] Yoon PJ, Fornes TD, Paul DR. *Polymer* 2003;44:5323.
- [89] Yoon PJ, Hunter DL, Paul DR. *Polymer* 2003;44:5341.
- [90] Fornes TD, Yoon PJ, Paul DR. *Polymer* 2003;44:7545.
- [91] Fornes TD, Hunter DL, Paul DR. *Polymer* 2004;45:2321.
- [92] Shah RK, Paul DR. *Polymer* 2004;45:2991.
- [93] Chavarria F, Paul DR. *Polymer* 2004;45:8501.
- [94] Fornes TD, Paul DR. *Macromolecules* 2004;37:7698.
- [95] Bourbigot S, Vanderhart D, Gilman J, Stretz HA, Paul DR. *Polymer* 2004;45:7627.
- [96] Hotta S, Paul DR. *Polymer* 2004;45:7639.
- [97] Ibanes C, David L, Seguela R, Rochas C, Robert G. *J Polym Sci Part B Polym Phys* 2004;42:2633–48.
- [98] Vlasveld DPN, Groenewold J, Bersee HEN, Mendes E, Picken SJ. *Polymer* 2005;46:6102–13.
- [99] Stretz HA, Paul DR, Li R, Keskkula H, Cassidy PE. *Polymer* 2005;46:2621.
- [100] Shah RK, Hunter DL, Paul DR. *Polymer* 2005;46:2646.
- [101] Stretz HA, Paul DR, Cassidy PE. *Polymer* 2005;46:3818.
- [102] Zeng QH, Yu AB, Lu GQ, Paul DR. *J Nanosci Nanotechnol* 2005;46:3818.
- [103] Lee H-S, Fasulo PD, Rodgers WR, Paul DR. *Polymer* 2005;46:11673.
- [104] Ahn YC, Paul DR. *Polymer* 2006;47:2830.
- [105] Shah RK, Paul DR. *Macromolecules* 2006;39:3327.
- [106] Lee H-S, Fasulo PD, Rodgers WR, Paul DR. *Polymer* 2006;47:3528.
- [107] Shah RK, Paul DR. *Polymer* 2006;47:4074.
- [108] Shah RK, Krishnaswamy RK, Takahashi S, Paul DR. *Polymer* 2006;47:6187.
- [109] Chavarria F, Paul DR. *Polymer* 2006;47:7760.
- [110] Stretz HA, Paul DR. *Polymer* 2006;47:8123.
- [111] Stretz HA, Paul DR. *Polymer* 2006;47:8527.
- [112] Shah RK, Cui L, Williams KL, Bauman B, Paul DR. *J Appl Polym Sci* 2006;102:2980.
- [113] Shah RK, Kim DH, Paul DR. *Polymer* 2007;48:1047.
- [114] Cui L, Paul DR. *Polymer* 2007;48:1632.
- [115] Chavarria K, Nairn K, White P, Hill AJ, Hunter DL, Paul DR. *J Appl Polym Sci* 2007;105:2910.
- [116] Yoo Y, Shah RK, Paul DR. *Polymer* 2007;48:4867.
- [117] Kim DH, Fasulo PD, Rodgers WR, Paul DR. *Polymer* 2007;48:5308.
- [118] Kim DH, Fasulo PD, Rodgers WR, Paul DR. *Polymer* 2007;48:5960.
- [119] Cui L, Ma X, Paul DR. *Polymer* 2007;48:6325.
- [120] Chavarria K, Shah RK, Hunter DL, Paul DR. *Polym Eng Sci* 2007;47:1847.
- [121] Liu L, Qi Z, Zhu X. *J Appl Polym Sci* 1999;71:1133–8.
- [122] Heinemann J, Reichert P, Thomann R, Mülhaupt R. *Macromol Rapid Commun* 1999;20:423–30.
- [123] Garcés JM, Moll DJ, Bicerano J, Fibiger R, McLeod DG. *Adv Mater* 2000;12(23):1835–9.
- [124] Varlot K, Reynaud E, Kloppfer MH, Vigier G, Varlet J. *J Polym Sci Part B Polym Phys* 2001;39:1360–70.
- [125] Reichert P, Hoffmann B, Bock T, Thomann R, Mülhaupt R, Friedrich C. *Macromol Rapid Commun* 2001;22(7):519–23.
- [126] Kim SW, Jo WH, Lee MS, Ko MB, Jho JY. *Polymer* 2002;43(3):103–11.
- [127] Ray SS, Yamada K, Ogami A, Okamoto M, Ueda K. *Macromol Rapid Commun* 2002;23:943–7.
- [128] Ray SS, Yamada K, Okamoto M, Fujimoto Y, Ogami A, Ueda K. *Polymer* 2003;44:6633–46.
- [129] Ray SS, Okamoto K, Okamoto M. *Macromolecules* 2003;36:2355–67.
- [130] Yalcin B, Valladares D, Cakmak M. *Polymer* 2003;44:6913–25.
- [131] Yalcin B, Cakmak M. *Polymer* 2004;45:2691–710.
- [132] Konishi Y, Cakmak M. *Polymer* 2005;46:4811–26.
- [133] Hsieh AJ, Moy P, Beyer FL, Madison P, Napadensky E. *Polym Eng Sci* 2004;44(5):825–37.
- [134] Weon J-I, Sue H-J. *Polymer* 2005;46:6325–34.
- [135] Vermogen A, Masenelli-Varlot K, Séguéla R, Duchet-Rumeau J, Boucard S, Prele P. *Macromolecules* 2005;38:9661–9.
- [136] Kim Y, White JL. *J Polym Sci* 2005;96:1888–96.
- [137] Morgan AB. *Polym Adv Technol* 2006;17:206–17.
- [138] Masenelli-Varlot K, Vigier G, Vermogen A, Gauthier C, Cavaillé JY. *J Polym Sci Part B Polym Phys* 2007;45:1243–51.
- [139] Picard E, Vermogen A, Gérard J-F, Espuche E. *J Membr Sci* 2007;292:133–44.
- [140] Krishnamoorti R. *MRS Bull* 2007;32:341.
- [141] Fornes TD, Hunter DL, Paul DR. *Macromolecules* 2004;37:1793.
- [142] Tanaka G, Goettler LA. *Polymer* 2002;43:541–53.
- [143] Kawasumi M, Hasegawa N, Kato M, Usuki A, Okada A. *Macromolecules* 1997;30:6333–8.
- [144] Hasegawa N, Kawasumi M, Kato M, Usuki A, Okada A. *J Appl Polym Sci* 1998;67:87–92.
- [145] Kato M, Okamoto H, Hasegawa N, Tsukigase A, Usuki A. *Polym Eng Sci* 2003;43(6):1312.
- [146] Hasegawa N, Usuki A. *J Appl Polym Sci* 2004;93:464–70.
- [147] Toth R, Coslanich A, Ferrone M, Ferraglia M, Priel S, Miertus S, et al. *Polymer* 2004;45:8075–83.
- [148] Százdli L, Pukánszky B, Földes E, Pukánszky B. *Polymer* 2005;46:8001–10.
- [149] Davis CH, Mathias LJ, Gilman JW, Schiraldi DA, Shields JR, Trulove P, et al. *J Polym Sci Part B Polym Phys* 2002;40:2661–6.
- [150] Vaia RA, Liu W. *J Polym Sci Part B Polym Phys* 2002;40:1590–600.
- [151] Morgan AB, Gilman JW. *J Appl Polym Sci* 2003;87:1329–38.
- [152] Lincoln DM, Vaia RA, Wang Z-G, Hsiao BS, Krishnamoorti R. *Polymer* 2001;42:9975–85.
- [153] Lincoln DM, Vaia RA, Wang Z-G, Hsiao BS. *Polymer* 2001;42:1621–31.
- [154] Vaia RA, Liu W, Koerner H. *J Polym Sci Part B Polym Phys* 2003;41:3214–36.
- [155] Justice RS, Schaefer DW, Vaia RA, Tomlin DW, Bunning TJ. *Polymer* 2005;46:4465–73.
- [156] Schaefer DW, Justice RS. *Macromolecules* 2007;40(24):8501–17.
- [157] VanderHart DL, Asano A, Gilman JW. *Chem Mater* 2001;13:3796–809.
- [158] VanderHart DL, Asano A, Gilman JW. *Chem Mater* 2001;13:3781–95.
- [159] VanderHart DL, Asano A. *Macromolecules* 2001;34:3819–22.
- [160] Davis RD, Gilman JW, VanderHart DL. *Polym Degrad Stab* 2003;79:111–21.
- [161] Ho DL, Briber RM, Glinka CJ. *Chem Mater* 2001;13:1923–31.
- [162] Schmidt G, Nakatani AI, Butler PD, Han CC. *Macromolecules* 2002;35:4725–32.
- [163] Oshinski AJ, Keskkula H, Paul DR. *Polymer* 1996;37(22):4891–907.
- [164] Corté L, Leibler L. *Polymer* 2005;46:6360–8.

- [165] Lee KY, Paul DR. *Polymer* 2005;46:9064.
- [166] Lee KY, Kim KH, Jeoung SK, Ju SI, Shim JH, Kim NH, et al. *Polymer* 2007;48:4174.
- [167] Mori T, Tanaka K. *Acta Metall* 1973;21:571.
- [168] Halpin JC, Kardos JL. *Polym Eng Sci* 1976;16(5):344.
- [169] Chow TS. *J Polym Sci* 1978;16:959–65.
- [170] Chow TS. *J Polym Sci* 1978;16:967–70.
- [171] Chow TS. *J Mater Sci* 1980;15:1873–88.
- [172] Hine PJ, Lusti HR, Gusev AA. *Compos Sci Technol* 2002;62:1445–53.
- [173] Lusti HR, Hine PJ, Gusev AA. *Compos Sci Technol* 2002;62:1927–34.
- [174] Van Es M, Xiqiao F, van Turnhout J, van der Giessen E. In: Al-Malaika S, Golovoy A, Wilkie CA, editors. *Specialty polymer additives: principles and applications*. Oxford: Blackwell Science; 2001. p. 391–414.
- [175] Brune DA, Bicerano J. *Polymer* 2002;43:369–87.
- [176] Luo J-J, Daniel IM. *Compos Sci Technol* 2003;63:1607–16.
- [177] Zhu L, Narh KA. *J Polym Sci Part B Polym Phys* 2004;42:2391–406.
- [178] Tsai J, Sun CT. *Compos Mater* 2004;38(7):567–79.
- [179] Sharaf MA, Mark JE. *Polymer* 2004;45:3943–52.
- [180] Wang J, Pyrz R. *Compos Sci Technol* 2004;64:925–34.
- [181] Wang J, Pyrz R. *Compos Sci Technol* 2004;64:935–44.
- [182] Shepard PD, Golemba FJ, Maine FW. *Adv Chem Ser* 1973;134:41–51.
- [183] Sheng N, Boyce MC, Parks DM, Rutledge GC, Abes JI, Cohen RE. *Polymer* 2004;45:487–506.
- [184] Hbaieb K, Wang QX, Chia YHJ, Cotterell B. *Polymer* 2007;48:901–9.
- [185] Sen S, Thomlin JD, Kumar SK, Koblinski P. *Macromolecules* 2007;40:4059–67.
- [186] Laura DM, Keskkula H, Barlow JW, Paul DR. *Polymer* 2002;43:4673–87.
- [187] Krishnamoorti R, Giannelis EP. *Macromolecules* 1997;30:4097–102.
- [188] Medellín-Rodríguez FJ, Burger C, Hsiao BS, Chu B, Vaia R, Phillips S. *Polymer* 2001;42:9015–23.
- [189] Wagener R, Reisinger TJG. *Polymer* 2003;44:7513–8.
- [190] Chen B, Evans JRG. *Scr Mater* 2006;54:1581–5.
- [191] Manevitch OL, Rutledge GC. *J Phys Chem B* 2004;108:1428–35.
- [192] Nielsen LE. *J Macromol Sci (Chem)* 1967;A1:929–42.
- [193] Lape NK, Nuxoll EE, Cussler EL. *J Membr Sci* 2004;236:29–37.
- [194] Gusev AA, Lusti HR. *Adv Mater* 2001;13:1641–3.
- [195] Fredrickson GH, Bicerano J. *J Chem Phys* 1999;110:2181–8.
- [196] Bharadwaj K. *Macromolecules* 2001;34:9189–92.
- [197] Kim SH, Kim SC. *J Appl Polym Sci* 2007;103:1262–71.
- [198] Choi WJ, Kim HJ, Yoon KH, Kwon OH, Hwang CI. *J Appl Polym Sci* 2006;100:4875–9.
- [199] Matayabas Jr JC, Turner SR. In: Pinnavaia TJ, Beall GW, editors. *Polymer–clay nanocomposites*. John Wiley & Sons Ltd.; 2000. p. 207–25; See also: Matayabas Jr JC, Turner SR, Sublett BJ, Connell GW, Gilmer JW, Barbee RB. US Patent 6,084,019, assigned to Eastman Chemical Corp.; July 4, 2000.
- [200] Sridhar V, Tripathy DK. *J Appl Polym Sci* 2006;101:3630–7.
- [201] Brulé B, Flat JJ. *Macromol Symp* 2006;233:210–6.
- [202] Triantafyllidis KS, LeBaron PC, Park I, Pinnavaia TJ. *Chem Mater* 2006;18:4393–8.
- [203] Zimmerman CM, Singh A, Koros WJ. *J Membr Sci* 1997;137:145–54.
- [204] Robeson LM. *J Membr Sci* 1991;62:165–85.
- [205] Husain S, Koros WJ. *J Membr Sci* 2007;288:195–207.
- [206] Chung TS, Jiang LY, Li Y, Kulprathipanja S. *Prog Polym Sci* 2007;32:483–507.
- [207] Matteucci S, Kusuma VA, Sanders D, Swinnea S, Freeman BD. *J Membr Sci* 2008;307:196–217.
- [208] Bourbigot S, Duquesne S, Jama C. *Macromol Symp* 2006;233:180–90.
- [209] Scharlt B, Bartholmai M, Knoll U. *Polym Adv Technol* 2006;17:772–7.
- [210] Nazare S, Kandola BK, Horrocks AR. *Polym Adv Technol* 2006;17:294–303.
- [211] Zanetti M, Camino G, Canavese D, Morgan AB, Lamelas FJ, Wilkie CA. *Chem Mater* 2002;14:189–93.
- [212] Lv JP, Liu WH. *J Appl Polym Sci* 2007;105:333–40.
- [213] Dasari A, Yu ZZ, Mai YW, Liu S. *Nanotechnology* 2007;18:445602 (1–10).
- [214] Kashiwagi T, Harris Jr RH, Zhang X, Briber RM, Cipriano BH, Raghavan SR, et al. *Polymer* 2004;45:881–91.
- [215] Qin H, Zhang S, Zhao C, Hu G, Yang M. *Polymer* 2005;46:8386–95.
- [216] Kashiwagi T, Du F, Winey KI, Groth KM, Shields JR, Bellayer SP, et al. *Polymer* 2005;46:471–81.
- [217] Kashiwagi T, Grulke E, Hilding J, Harris R, Awad W, Douglas J. *Macromol Rapid Commun* 2002;23:761–5.
- [218] Ray SS, Bousmina M. *Macromol Rapid Commun* 2005;26:450–5.
- [219] Li Y, Shimizu H. *Polymer* 2004;45:7381–8.
- [220] Khatua BB, Lee DJ, Kim HY, Kim JK. *Macromolecules* 2004;37:2454–9.
- [221] Si M, Araki T, Ade H, Kilcoyne ALD, Fisher R, Sokolov JC, et al. *Macromolecules* 2006;39:4793–801.
- [222] Vo LT, Giannelis EP. *Macromolecules* 2007;40:8271–6.
- [223] Zhang Q, Yang H, Fu Q. *Polymer* 2004;45:1913–22.
- [224] Wang Y, Zhang Q, Fu Q. *Macromol Rapid Commun* 2003;24:231–5.
- [225] Hung HS, Hsu SH. *Nanotechnology* 2007;18:475101 (9 pp).
- [226] Chen CZ, Cooper SL. *Adv Mater* 2000;12:843–6.
- [227] Damm C, Müntstedt H, Rösch A. *Mater Chem Phys* 2008;108:61–6.
- [228] Alt V, Bechert T, Steinrück P, Wagener M, Seidel P, Dingeldein E, et al. *Biomaterials* 2004;25:4383–91.
- [229] Hule RA, Pochan DJ. *MRS Bull* 2007;32:354–8.
- [230] Kim HW, Kim HE, Salih V. *Biomaterials* 2005;26:5221–30.
- [231] Huang J, Lin YW, Fu XW, Best SM, Brooks RA, Rushton N, et al. *J Mater Sci Mater Med* 2007;18:2151–7.
- [232] Lee YH, Lee JH, An IG, Kim C, Lee DS, Lee YK, et al. *Biomaterials* 2005;26:3165–72.
- [233] Zhang Q, Zha L, Ma J, Liang B. *Macromol Rapid Commun* 2007;28:116–20.
- [234] Haraguchi K, Li HJ. *Macromolecules* 2006;39:1898–905.
- [235] Gupta AK, Gupta M. *Biomaterials* 2005;26:3995–4021.
- [236] Berry CC. *J Mater Chem* 2005;15:543–7.
- [237] Toprak MS, McKenna BJ, Waite JH, Stucky GD. *Chem Mater* 2007;19:4263–9.
- [238] Vadala ML, Rutnakornpituk M, Zalich MA, Pierre St TG, Riffle JS. *Polymer* 2004;45:7449–61.
- [239] Rutnakornpituk M, Baranauskas VV, Riffle JS, Connolly J, Pierre St TG, Dailey JP. *Eur Cells Mater* 2002;3:102–5.
- [240] Rolland JP, Maynor BW, Euliss LE, Exner AE, Denison GM, Desimone JM. *J Am Chem Soc* 2005;127:10096–100.
- [241] Kongkanand A, Kuwabata S, Girishkumar G, Kamat P. *Langmuir* 2006;22:2392–6.
- [242] DeLuca NW, Elabd YA. *J Polym Sci Part B Polym Phys* 2006;44:2201–25.
- [243] Kim YS, Wang F, Hickner M, Zadwodzinski TA, McGrath JE. *J Membr Sci* 2003;212:263–82.
- [244] Zaidi SMJ, Mikhailenko SD, Robertson GP, Guiver MD, Kaliaguine S. *J Membr Sci* 2000;173:17–34.
- [245] Wang Z, Ni H, Zhao C, Li X, Fu T, Na H. *J Polym Sci Part B Polym Phys* 2006;44:1967–78.
- [246] Li X, Xu D, Zhang G, Wang Z, Zhao C, Na H. *J Appl Polym Sci* 2007;103:4020–6.
- [247] Su YH, Liu YL, Sun YM, Lai JY, Guiver MD, Gao Y. *J Power Sources* 2006;155:111–7.
- [248] Jiang R, Kunz HR, Fenton JM. *J Membr Sci* 2006;272:116–24.
- [249] Yang C, Srinivasan S, Arico AS, Creti P, Baglio V, Antonucci V. *Electrochem Solid-State Lett* 2001;4:A31–4.
- [250] Hill ML, Kim YS, Einsla BR, McGrath JE. *J Membr Sci* 2006;283:102–8.
- [251] Prashantha K, Park SG. *J Appl Polym Sci* 2005;98:1875–8.
- [252] Bébin P, Caravanier M, Galiano H. *J Membr Sci* 2006;278:35–42.
- [253] Thomassin JM, Pagnoulle C, Bizzari D, Caldarella G, Germain A, Jérôme R. *Solid State Ionics* 2006;177:1137–44.
- [254] Barroso-Bujans F, Verdejo R, Arroyo M, Lopez-Gonzalez MM, Riande E, Lopez-Manchado MA. *Macromol Rapid Commun* 2008;29:234–8.
- [255] Baibarac M, Gómez-Romero P. *J Nanosci Nanotechnol* 2006;6:1–14.
- [256] Baughman RH, Zakhidov AA, De Heer WA. *Science* 2002;297:787–92.
- [257] Moniruzzaman M, Winey KI. *Macromolecules* 2006;39:5194–205.
- [258] Sandler JKW, Kirk JE, Kinloch IA, Shaffer MSP, Windle AH. *Polymer* 2003;44:5893–9.
- [259] Brynning MB, Islam MF, Kikkawa JM, Yodh AG. *Adv Mater* 2005;17:1186–91.
- [260] Kim YS, Wright JB, Grunlan JC. *Polymer* 2008;49:570–8.
- [261] Huynh WU, Dittmer JJ, Alivisatos AP. *Science* 2002;295:2425–7.
- [262] Liang Z, Dzienis KL, Xu J, Wang Q. *Adv Funct Mater* 2006;16:542–8.
- [263] Qi XY, Pu KY, Fang C, Wen GA, Zhang H, Boey FYC, et al. *Macromol Chem Phys* 2007;208:2007–17.
- [264] Olson DC, Shaheen SS, Collins RT, Ginley DS. *J Phys Chem C* 2007;111:16670–8.
- [265] Kwong CY, Choy WCH, Djurišić AB, Chui PC, Cheng KW, Chan WK. *Nano-technology* 2004;15:1156–61.
- [266] Kymakis E, Amarantunga GAJ. *Appl Phys Lett* 2002;80:112–5.
- [267] Tekin E, Smith PJ, Hoepfener S, van den Berg AMJ, Susa AS, Rogach AL, et al. *Adv Funct Mater* 2007;17:23–8.
- [268] Park JW, Ullah MH, Park SS, Ha CS. *J Mater Sci Mater Electron* 2007;18:5393–7.
- [269] Oey CC, Djurišić AB, Kwong CY, Cheung CH, Chan WK, Nunzi JM, et al. *Thin Solid Films* 2005;492:253–8.
- [270] Park JH, Lim YT, Park OO, Kim JK, Yu JW, Kim YC. *Chem Mater* 2004;16:688–92.
- [271] Park JH, Lim YT, Park OO, Kim YC. *Macromol Rapid Commun* 2003;24:331–4.
- [272] Park JH, Lim YT, Park OO, Kim JK, Yu JW, Kim YC. *Adv Funct Mater* 2004;14:377–82.
- [273] Miyake J, Chujo Y. *Macromol Rapid Commun* 2008;29:86–92.
- [274] Stankovich S, Dikin DA, Dommett GHB, Kohlhaas KM, Zimney EJ, Stach EA, et al. *Nature* 2006;442:282–6.
- [275] Novoselov KS, Geim AK, Morozov SV, Jiang D, Zhang Y, Dubonos SV, et al. *Science* 2004;306:666–9.
- [276] Gilje S, Han S, Wang M, Wang KL, Kaner RB. *Nano Lett* 2007;7:3394–8.
- [277] Van Noorden R. *Nature* 2006;442:228–9.
- [278] Hatchett DW, Josowicz M. *Chem Rev* 2008. on web 01/03/2008.
- [279] Kong J, Franklin NR, Zhou C, Chapline MG, Peng S, Cho K, et al. *Science* 2000;287:622–5.
- [280] An KH, Jeong SY, Hwang HR, Lee YH. *Adv Mater* 2004;16:1005–9.
- [281] Ali SR, Ma Y, Parajuli RR, Balogun Y, Lai WYC, He H. *Anal Chem* 2007;79:2583–7.
- [282] Feng X, Mao C, Yang G, Hou W, Zhu JJ. *Langmuir* 2006;22:4384–9.
- [283] Zhang M, Fang S, Zakhidov AA, Lee SB, Aliev AE, Williams CD, et al. *Science* 2005;309:1215–9.
- [284] Vaia RA, Maguire JF. *Chem Mater* 2007;18:2736–51.



Donald R. Paul holds the Ernest Cockrell, Sr. Chair in Engineering at the University of Texas at Austin and is also the Director of the Texas Materials Institute. He received degrees in Chemical Engineering from North Carolina State University (B.S.) and the University of Wisconsin (M.S. and Ph.D.) and then worked at the Chemstrand Research Center for two years. He joined the Department of Chemical Engineering at the University of Texas at Austin in 1967 where he served as Department Chairman during 1977–1985. His research has involved various aspects of polymer blends, membranes for separation, drug delivery, packaging, processing, and nanocomposites. His interests in nanocomposites include developing strategies for exfoliation of clays in polymers by melt processing and understanding the properties of the resulting materials. Synthesis, characterization, and performance are all integral parts

of these research programs. He has edited numerous books on blends and membranes and has published approximately 570 research papers. He has received awards for teaching, research, and leadership from the University of Texas, ACS, AIChE, SPE, and the Council for Chemical Research. He has been designated a distinguished graduate of North Carolina State University and of the University of Wisconsin. He was elected to the National Academy of Engineering in 1988 and to the Mexican Academy of Sciences in 2000. He has served as Editor of *Industrial and Engineering Chemistry Research*, published by ACS, since 1986.



Lloyd M. Robeson received his B.S. in Chemical Engineering in 1964 (Purdue University) and his Ph.D. also in Chemical Engineering in 1967 (University of Maryland). He worked for Union Carbide from 1967 to 1986 and for Air Products and Chemicals, Inc. from 1986 to 2007 from where he retired last year. He is presently an Adjunct Professor at Lehigh University. His entire career has been involved with polymer science research and development with emphasis on polymer blends, membrane separation, physical property characterization of polymers, polymer permeability, polymer composites, polymers for emerging technologies and commercialization of a number of new polymers, polymer blends and composites. He is the (co)author of over 95 US Patents and over 95 publications. He is a member of the National Academy of Engineering. His awards include the Applied Polymer Science award of ACS, Industrial

Polymer Scientist award of the Polymer Division of ACS, induction into the Engineering Innovation Hall of Fame at University of Maryland, and several distinguished alumni awards from Purdue University and the University of Maryland. He is the coauthor of a book titled "Polymer–Polymer Miscibility" (1979) and the author of a book titled "Polymer Blends: A Comprehensive Review" (2007).